SLAC-PUB-1455
(T) (E)
July, 1974

DEEP INELASTIC SCATTERING AND THE STRUCTURE OF HADRONS*

Frederick J. Gilman
Stanford Linear Accelerator Center, Stanford University, Stanford, California 94305

Rapporteur's Talk
XVII International Conference on High Energy Physics
London, England
July 1-10, 1974

* Supported by the U. S. Atomic Energy Commission.

I. Introduction

When this conference was last held in Western Europe in 1968, the first preliminary results on deep inelastic electron-proton scattering were given. The $\theta = 6^{\circ}$ data, as presented by the SLAC MIT collaboration to the Vienna Conference[1] are shown in Fig. 1, where an indication of the scaling behavior predicted by Bjorken[2] is already in evidence.

This year, final results from a second experiment on 6° and 10° electron scattering on both hydrogen and deuterium targets were published,[3] as shown in Fig. 2. Aside from the vast improvement in the accuracy, quantity, and scope of the data on deep inelastic lepton scattering in the intervening six years, there has been a qualitative change of great importance in our understanding of both nucleon structure and weak and electromagnetic currents as a result of these and related experiments. A well-investigated theoretical framework has grown up, within which the data may be interpreted, and from which additional predictions and speculations may be made. The ideas of scaling, the light cone behavior of products of currents, and the quark-parton model generated thereby have come to occupy such an important place in high energy physics that they effect aspects of the subject matter of almost every session at this conference.

Moreover, this conference has seen the presentation both from SLAC and NAL of new deep inelastic lepton scattering data with more than an order of magnitude higher energy and/or momentum transfer squared than characterizes the data in Fig. 1. As such, it is an excellent time to review where we stand in understanding deep inelastic scattering and what has been revealed thereby about the structure of hadrons. We do so with an eye as to how the previously successful

abstraction from the free quark model of certain properties of current commutators might be modified as we enter this new domain of energies and momentum transfers.

II. Kinematic and Theoretical Framework

Inelastic lepton scattering has the very important conceptual and practical advantage that one can use the current-current form of the weak or electromagnetic interaction in lowest order to separate the double differential cross section for detection of only the final lepton,[4]

$$\frac{d^2\sigma}{d\Omega' dE'} \propto L_{\mu\nu} W_{\mu\nu} , \tag{1}$$

into a known part arising from the lepton trace, $L_{\mu\nu}$, and a structure tensor for the hadron target, $W_{\mu\nu}$. For inelastic electron or muon scattering $W_{\mu\nu}$ is defined as

$$W_{\mu\nu} = \left(\frac{1}{2\pi e^2}\right) \overline{\sum_{\text{spin}}} \int dx^4 e^{-iq\cdot x} < p \,|\, [J_\mu^{em}(x), J_\nu^{em}(0)] \,|\, p > . \tag{2}$$

Lorentz and gauge invariance permit the tensor to be written in this case as

$$W_{\mu\nu} = W_1(\nu, q^2)\left(\delta_{\mu\nu} - \frac{q_\mu q_\nu}{q^2}\right) + W_2(\nu, q^2)\left(p_\mu - \frac{p\cdot q}{q^2} q_\mu\right)\left(p_\nu - \frac{p\cdot q}{q^2} q_\nu\right) \Big/ M^2 \tag{3}$$

where the familiar Lorentz scalar structure functions W_1 and W_2 depend on $\nu = -p\cdot q/M$ and q^2, the laboratory energy and invariant momentum transfer squared carried by the virtual photon.

We will be considering the limit where both ν and q^2 become large, for which the region of configuration space $x^2 \simeq 0$, i.e. the light cone,[5] is the important domain of integration in Eq. (2). For the purpose of studying this, it is relevant to consider the Wilson expansion for operator products at short distances,[6]

$$\left[J_\mu^{em}(x), J_\nu^{em}(0)\right] = \sum_{n=0}^{\infty} S_n(x)\, O_{\mu\nu\mu_1,\ldots\mu_{2n}}(0)\, x_{\mu_1}\ldots x_{\mu_{2n}} + \text{other terms}, \tag{4}$$

where $S_n(x)$ is a singular c-number function and we have only written the leading term[7] contributing to W_2 in the large ν and q^2 limit. Taking the spin-averaged hadronic matrix element of Eq. (4) in the limit of large q^2 (with corresponding neglect of non-leading terms), one finds from Eq. (2) that the moment

$$M_n(q^2) \equiv \int_1^\infty \frac{d\omega}{\omega^{2n+2}}\, \nu W_2(\nu, q^2) = c_n \tilde{S}_n(q^2), \tag{5}$$

where $\tilde{S}_n(q^2)$ is essentially the Fourier transform of $S_n(x)$ and c_n is a constant related to the hadronic matrix element of $O_{\mu\nu\mu_1\ldots\mu_{2n}}(0)$, while ω is the familiar scaling variable,

$$\omega = 2M\, \nu/q^2 . \tag{6}$$

As the c_n's are constants, the character of the behavior of νW_2 as ν and q^2 become large is seen to correspond directly to the behavior of the $\tilde{S}_n(q^2)$'s as $q^2 \to \infty$. Their behavior is a characteristic of that of the product of two currents at short distances — all information about the specific hadron target is separated and contained in the c_n's. For the moments, $M_n(q^2)$, and the

corresponding functions $S_n(q^2)$, the following possibilities present themselves:

1. The moments behave as

$$M_n(q^2) \xrightarrow[q^2 \to \infty]{} c_n(\mu^2/q^2)^{d_n}, \tag{7}$$

where d_n is called the anomalous dimension. Such a behavior is common to many interacting field theories in ladder approximation. The d_n's are monotonically increasing functions of n. Since a candidate for $O_{\mu\nu\mu_1 \cdots \mu_{2n}}(0)$ in the case $n=0$ is the stress-energy tensor with vanishing anomalous dimension, the first term in Eq. (4) is usually taken to have $d_0 = 0$. As a result

$$M_0(q^2) \equiv \int_1^\infty \frac{d\omega}{\omega^2}\, \nu W_2(\nu, q^2) \equiv \int_0^1 dx\ \nu W_2(\nu, q^2) \xrightarrow[q^2 \to \infty]{} c_0, \tag{8}$$

where $x = 1/\omega$; i. e. the area under νW_2 is constant at large q^2.

2. Certain non-Abelian gauge theories are asymptotically free,[8,9] in that the "effective coupling constant" vanishes logarithmically as $q^2 \to \infty$. In such theories the moments behave as

$$M_n(q^2) \xrightarrow[q^2 \to \infty]{} c_n \left[\frac{1}{\ln(q^2/\mu^2)}\right]^{A_n}. \tag{9}$$

In a crude sense such theories then almost scale, i. e. scaling of the moments is only broken logarithmically. The constants A_n are determined by the pertinant gauge group and the fermion representation chosen.[8,9]

3. If all the functions $\tilde{S}_n(q^2)$ approach finite non-zero limits as $q^2 \to \infty$, then the $S_n(x)$ have the canonical form characteristic of free field theory. This

is just the condition of Bjorken scaling,[2] for if all moments approach non-zero constants as $q^2 \to \infty$, then νW_2 is a function only of $\omega = 1/x$ rather than ν and q^2 independently as $\nu, q^2 \to \infty$.

To gain further information on the commutator of two currents when scaling obtains, we abstract from the free quark model, where one finds for the leading singularity on the light cone[5,10]

$$\left[V_\mu^\alpha(x), V_\nu^\beta(0)\right] \underset{x^2=0}{\sim} \left\{\frac{1}{4\pi}\partial_\lambda\left[\epsilon(x_0)\,\delta(x^2)\right]\right\}.$$

$$\Big\{ i f^{\alpha\beta\gamma}\Big[\Big(V_\nu^\gamma(x,0) + V_\nu^\gamma(0,x)\Big)\delta_{\mu\lambda} + \Big(V_\mu^\gamma(x,0) + V_\mu^\gamma(0,x)\Big)\delta_{\nu\lambda} - \Big(V_\lambda^\gamma(x,0) + V_\lambda^\gamma(0,x)\Big)\delta_{\mu\nu}$$

$$+ i\epsilon_{\mu\nu\lambda\sigma}\Big(A_\sigma^\gamma(x,0) - A_\sigma^\gamma(0,x)\Big)\Big] + d^{\alpha\beta\gamma}\Big[\Big(V_\nu^\gamma(x,0) - V_\nu^\gamma(0,x)\Big)\delta_{\mu\lambda} + \Big(V_\mu^\gamma(x,0) - V_\mu^\gamma(0,x)\Big)\delta_{\nu\lambda}$$

$$- \Big(V_\lambda^\gamma(x,0) - V_\lambda^\gamma(0,x)\Big)\delta_{\mu\nu} - i\epsilon_{\mu\nu\rho\sigma}\Big(A_\sigma^\gamma(x,0) + A_\sigma^\gamma(0,x)\Big)\Big]\Big\}, \tag{10}$$

where $V_\mu^\alpha(x)$ and $A_\mu^\alpha(x)$ are the vector and axial-vector currents with SU(3) index α and

$$V_\mu^\alpha(x,0) = :\bar{\psi}(x)(\lambda^\alpha/2)\, i\gamma_\mu\psi(0): \text{ and } A_\mu^\alpha(x,0) = :\bar{\psi}(x)(\lambda^\alpha/2)\, i\gamma_\mu\gamma_5\psi(0): \tag{11}$$

are bilocal operators. Similar expressions obtain[5,10] for the commutator of a vector and an axial-vector, $\left[V_\mu^\alpha(x), A_\nu^\beta(0)\right]$, or two axial-vector currents, $\left[A_\mu^\alpha(x), A_\nu^\beta(0)\right]$, relevant in weak interactions, while the connection to electromagnetic processes is made on recalling that

$$J_\mu^{em}(x) = e\left[V_\mu^3(x) + \left(\frac{1}{\sqrt{3}}\right) V_\mu^8(x)\right] . \tag{12}$$

Some important characteristics of Eq. (10) are that:

1. The free field c-number singularity is explicit in the first factor, yielding scaling of W_1, νW_2, and (in neutrino scattering) νW_3. Comparison with the Wilson expansion, Eq. (4), shows that the operators $O_{\mu\nu\mu_1\ldots\mu_{2n}}(0)$ are essentially the coefficients of a Taylor series expansion of the bilocal operators $V_\mu^\alpha(x,0)$ and $A_\mu^\alpha(x,0)$.

2. The Lorentz structure of the tensor indices reflects the spin $\frac{1}{2}$ nature of the quark fields and results in

$$\left(\frac{2M}{\omega}\right) W_1 = \nu W_2 , \tag{13}$$

which corresponds to the vanishing of the longitudinal relative to transverse cross sections.

3. The SU(3) indices of the currents are explicit in terms of the SU(3) structure constants $f^{\alpha\beta\gamma}$ and $d^{\alpha\beta\gamma}$. This leads to relations between neutrino and electron scattering which we will consider later, as well as restrictions like[11]

$$\tfrac{1}{4} \leq \frac{\sigma_{en}}{\sigma_{ep}} \leq 4 . \tag{14}$$

4. Matrix elements of the bilocals determine the shape, as a function of ω, of W_1, νW_2, and νW_3. A picturesque equivalent of this quark light cone algebra is in terms of the quark parton model[12,13]. Here one regards the nucleon target as being composed of point constituents whose interaction with the lepton

can be treated in impulse approximation in an infinite momentum frame. Each type (i) of quark or anti-quark, with charge Q_i (in units of e), is taken to have a distribution $f_i(x)$ in the fractional longitudinal momentum $x = p_z^{(parton)}/p_z^{(nucleon)}$. Then for deep inelastic electroproduction,

$$\nu W_2 = \Sigma_i Q_i^2 x f_i(x) = 2MxW_1 , \tag{15}$$

where x is both the fractional momentum of the struck parton and the value of the scaling variable $q^2/2M\nu = 1/\omega$. With arbitrary $f_i(x)$'s, Eq. (15) is just a rewriting of the appropriate Fourier transform of matrix elements of Eq. (10). Properties 1 through 4 are all mixed up together in the parton model. In the following we shall try and examine each of these properties in turn, using the new data and in the light of recent theoretical work.

III. Scaling and its Breaking

First let us take up the question of the nature of the leading singularity. Here we immediately also face the size of non-leading terms, something which is much less under theoretical control than the nature of the leading singularity. One expression of this is in terms of scaling variables. Defining

$$\omega' = \omega + M^2/q^2 , \tag{16}$$

we see that the leading light cone behavior is the same if there is "scaling" in either ω or ω', for clearly $\omega' \to \omega$ as $q^2 \to \infty$. However at finite q^2 there are appreciable differences in considering the structure functions as they depend on q^2 with either ω or ω' fixed. For example, if $\nu W_2 = c(\omega' - 1)^3$ for $q^2 \geq 1\ \mathrm{GeV}^2$

and $\omega' < 2$, then νW_2 at fixed $\omega = 1.5$ decreases by almost a factor of two between $q^2 = 8\ \mathrm{GeV}^2$ and ∞. Of course, where νW_2 is approximately constant as a function of ω, the choice of scaling variable makes little difference — a constant scales in any variable.

This question is well illustrated in a paper from the MIT-SLAC Spectrometer Facilities Group collaboration[14] submitted to this conference. Using an experimental separation of νW_2 and W_1, they determine their q^2 dependence at fixed ω, as shown in Fig. 3. Parametrizing the observed q^2 dependence in terms of a factor $(1 - 2q^2/\Lambda_i^2)$, they find for $1.5 < \omega < 3$ that

$$\Lambda_2^2 = 75 \pm 7\ \mathrm{GeV}^2 \quad \text{and} \quad \Lambda_1^2 = 62 \pm 9\ \mathrm{GeV}^2 \ . \tag{17}$$

This fall of νW_2 (or W_1) with increasing q^2 for fixed ω near 1 has been known for some time.[15] But at fixed ω', Λ_i^2 is consistent with infinity, with 95% confidence lower limits being

$$\Lambda_2^2 > 179\ \mathrm{GeV}^2 \quad , \quad \Lambda_1^2 > 84\ \mathrm{GeV}^2 \ . \tag{18}$$

This just corresponds to the familiar scaling in ω', as shown from earlier SLAC-MIT results[15] in Fig. 4. Scaling in one variable implies a definite manner of approach to scaling in another variable, if both agree as $q^2 \to \infty$.

In another single arm experiment submitted to this conference, W. B. Atwood et al.[16] at SLAC have investigated inelastic electron scattering at large angles, 50° and 60°, using the 1.6 GeV spectrometer, while simultaneously extending the small angle measurements with the 20 GeV spectrometer. Analysis of the data gathered, extending out to $q^2 = 33\ \mathrm{GeV}^2$ for electron scattering from hydrogen and deuterium, is still very preliminary.

Some results from a comparison of 13.9 GeV electron and positron scattering were reported, as shown in Fig. 5. No significant difference between electron and positron deep inelastic scattering is seen out to $q^2 = 15\ \mathrm{GeV}^2$. As well as supporting the dominance of one photon exchange in deep inelastic scattering (the real part of a two photon amplitude may interfere with the one photon amplitude to produce a difference between e^+p and e^-p inelastic scattering), such data limit the size of some direct lepton-hadron interactions proposed to explain e^+e^- annihilation data.[17]

Results from a preliminary analysis of the 50° and 60° data were discussed in the parallel session. The cross section at such large angles is dominated by contributions from the structure function W_1. A fair approximation to the data for W_1 over almost three orders of magnitude of change from $\omega' \simeq 2.5$ down to $\omega' \simeq 1.15$ is given by taking a fit for $\nu W_2(\omega')$ and assuming $\sigma_L/\sigma_T = 0.18$ to calculate values for W_1. However, there is some spread of data points with q^2 at fixed values of ω' beyond that calculated with the above assumptions for νW_2 and σ_L/σ_T. A careful study of all the data is needed to study simultaneously possible variations of σ_L/σ_T and scaling of νW_2 and W_1, as well as possible systematic errors for each of the experiments.

Tests of scaling in high energy muon deep inelastic scattering at FNAL have been reported to this conference by D. J. Fox et al.[18] using muon beams of 56.3 and 150 GeV impinging on an iron target. In an ingenious and direct test of scaling, the apparatus shown in Fig. 6 is "scaled" in such a way that muons corresponding to values of ν and q^2 each scaled by the ratio of the incident energies (and hence corresponding to the same value of ω) pass through the same positions in the spectrometer magnets and spark chambers, thereby

minimizing possible systematic errors. Alternately, a comparison of data at either energy may be made with Monte Carlo predictions based on SLAC results.

The data at 56.3 GeV was gathered in April of this year and the results of the direct test of scaling are preliminary. Because of showers in the front spark chambers and proportional chambers due to hadrons from high multiplicity events, only information from downstream of the first spectrometer magnet is used in the present analysis, decreasing the resolution from $\simeq 13\%$ to $\simeq 18\%$ in $1/E'$. The additional information is believed to be recoverable and will be incorporated in a later analysis.

The ratio of 150 GeV data to 56.3 GeV data is shown in Fig. 7f with statistical errors only. The fit of this ratio to the form $N/(1+q^2/\Lambda^2)^2$ gives

$$N = 1.10 \pm 0.10 , \qquad 1/\Lambda^2 = 0.0120 \pm 0.0060 \text{ GeV}^{-2} ,$$

a two standard deviation effect. A fit with $1/\Lambda^2 = 0$ has a 12% confidence level. The effect of various changes due to radiative corrections, variation of σ_L/σ_T, worse momentum resolution, and a shift in the final muon's momentum are shown in Fig. 8.

Note also that the average value of ω changes with q^2 from ≈ 16 in the lowest q^2 bin to ≈ 2 in the highest. On the theoretical side, if scaling were to hold in ω' rather than ω (as for the SLAC-MIT data), one expects a drop of 10 to 15% at fixed $\omega = 2$ between the two q^2 values characterizing the last bin. The evidence for a breakdown of "scaling" based on the preliminary data for the ratio of 150 GeV to 56.3 GeV data is not strong, taken by itself.

A stronger statement is made in Ref. 18 based on taking the ratio of the 150 GeV data to a Monte Carlo calculation based on a fit to SLAC-MIT data, as

shown in Fig. 7g. A fit to the same functional form as before gives

$$N = 1.30 \pm 0.06 \ , \quad 1/\Lambda^2 = 0.0083 \pm 0.0015 \ \mathrm{GeV}^{-2}$$

where the estimated systematic error in N is $\pm$ 0.10 and in $1/\Lambda^2$ is $\pm$ 0.0030 GeV^{-2}. The observed deviation is > 1 at low q^2 (and high ω) and < 1 at high q^2 (and low ω). Note that for $\omega \gtrsim 10$, one is actually extrapolating beyond the SLAC data used in the fit. In the region of overlap in ω and q^2 with SLAC there is agreement to $\pm$ 5%. If one cuts out events with $\omega > 9$, then Fig. 7h results. The value of $1/\Lambda^2$ is reduced by a factor of two and $N = 1.1 \pm 0.1$. The claimed rise with q^2 at large ω and fall at small ω is evidence against a functional form like $N/(1+q^2/\Lambda^2)^2$, but welcome in asymptotically free gauge theories, as we shall see in a moment.

Further information on scaling is available from the deep inelastic neutrino scattering experiments submitted to this conference. Recall that in terms of the variables

$$x = 2M\nu/q^2 \quad \text{and} \quad y = \nu/E \ , \tag{19}$$

one may write the double differential inelastic cross section in the high energy limit as

$$\frac{d^2\sigma(\nu,\bar{\nu})}{dx\,dy} = \left(\frac{G^2ME}{\pi}\right)\left[(1-y)\,\nu W_2 + \frac{y^2}{2}\ (2Mx)\ W_1 \mp y(1-\tfrac{1}{2}y)x\,\nu W_3)\right] , \tag{20}$$

where $G = 1.0 \times 10^{-5}/M_N^2$ is the weak coupling constant. Assuming scaling of $W_1 = F_1(x)$, $\nu W_2 = F_2(x)$, and $\nu W_3 = F_3(x)$ implies that

$$\sigma_{TOT}^{(\nu,\bar{\nu})}(E) = \left(\frac{G^2ME}{\pi}\right)\int_0^1 dx\left[\frac{F_2(x)}{2} + \frac{2MxF_1(x)}{6} \mp \frac{xF_3(x)}{3}\right] , \tag{21}$$

and a consequent linear rise in the total cross section with incident beam energy E.

The agreement of data from Gargamelle with this is discussed elsewhere.[19,20] In new experiments submitted to this conference, the Caltech-NAL[21] and Harvard-Pennsylvania-Wisconsin[22] collaborations, both working at FNAL, have reported total cross section results for both neutrinos and antineutrinos. The results[21] of the Caltech-NAL experiment using a dichromatic beam with $< E >$ of 38 and 108 GeV are shown in Fig. 9. The broad-band beam used in the Harvard-Pennsylvania-Wisconsin experiment[22] gives results which are shown in Figs. 10 and 11. Both these experiments show consistency with a continuing linear rise of the total cross section with E for both neutrinos and antineutrinos for beam energies into the 100 to 200 GeV range.

A more stringent test of scaling is provided by considering the q^2 distribution, and more specifically

$$< q^2 > = 2ME < xy > \tag{22}$$

where

$$< f(x,y) > = \frac{\iint dx\,dy \frac{d^2\sigma}{dx\,dy} f(x,y)}{\iint dx\,dy \frac{d^2\sigma}{dx\,dy}} .$$

Thus $< q^2 >$ should also rise linearly with E if there is scaling, with a coefficient related to the first moment of $F_2(x)$, $2MxF_1(x)$ and $xF_3(x)$, i.e.

$$\int_0^1 dx\; x\,F_2(x), \quad \text{etc.}$$

Figures 12 and 13 show this predicted linear rise in $< q^2 >$ compared with the Harvard-Pennsylvania-Wisconsin data[22] extending up to ≈ 200 GeV. Alternately one may look at the q^2 distribution, as done by the Caltech-NAL group,[21] and shown in Fig. 14. In terms of a multiplicative propagator term $\left[1 + q^2/\Lambda^2\right]^{-2}$, the agreement between experiment and expectation based on $F_2^{ed}(x)$ from SLAC yields a 90% confidence lower limit

$$\Lambda > 10.3 \text{ GeV} ,$$

with values of Λ from 15 GeV to infinity equally likely.

An even stronger test of scaling is made by integrating over y and comparing directly $d\sigma^{(\nu,\bar{\nu})}/dx$ with $F_2^{ed}(x)$, under the assumption that $F_2(x)$, $2Mx\,F_1(x)$ and $x\,F_3(x)$ are proportional — something we will see evidence for later. The resulting comparison is shown in Fig. 15 for the Caltech-NAL data and in Fig. 16 for those from the Harvard-Pennsylvania-Wisconsin experiment. Within errors there is no indication of a deviation from scaling as seen at SLAC.

Throughout the above discussion we saw comparisons have been made by experimentalists to a breakdown of scaling in the form $\left[1 + q^2/\Lambda^2\right]^{-2}$. Such a form was suggested by Chanowitz and Drell[23] in the guise of a parton form factor. This idea was extended by West,[24] who adds a quark anomalous moment term, permitting a cancellation in the space-like region (and approximate scaling in electroproduction) and an enhancement for time-like q^2 (to explain e^+e^- annihilation). While this is more a phenomenology than a complete field theory of scaling and its breakdown, it is at least a useful parametrization in certain regions. In addition to an obvious effect on q^2 distributions, the presence of such extra q^2 dependent factors has important effects on other

distributions, particularly for deep inelastic neutrino scattering. An example, from the recent paper of West and Zerwas[25], is shown in Fig. 17. On the basis of the neutrino data we saw earlier, the specific non-zero values[24] of the quark magnetic moment and $1/\Lambda^2$ used in Fig. 17 (and taken from fitting[23,24] inelastic electron scattering and $\sigma_T(e^+e^- \to \text{hadrons})$) would seem ruled out.[26]

The question of scale breaking in parton models has been reviewed in the parallel session by Professor Polkinghorne.[27] In addition, he pointed out the existence of non-leading terms which behave like $1/\nu^{\epsilon}$ (or $(1/q^2)^{\epsilon}$) with $\epsilon < \frac{1}{2}$ in a class of parton models which yield scaling and large multiplicities.[28]

From a field theoretic viewpoint, one would like to investigate the behavior of the moments,

$$M_n(q^2) \equiv \int_0^1 dx\, x^{2n}\, \nu W_2(\nu, q^2)$$

as $q^2 \to \infty$ and compare with the behavior expected in Eqs. (7) and (9). Unfortunately, the data only extend up to finite values of $\omega = 1/x$ at any given q^2, so it is impossible in principle to obtain the actual moment purely experimentally. An evaluation of the moments using ω' and integrating up to $\omega' = 5$ was reported by Bloom[29] at the Bonn Conference. If interpreted in terms of anomalous dimensions, rather small values (0 to ≈ 0.15) resulted up to $n = 3$. This analysis has been recently redone by Nachtmann[30] in a way which isolates the contribution of only the leading term in the Wilson expansion. Larger values of the fitted anomalous dimensions result, e.g. $d_1 \approx 0.3$.

Even without actually calculating the moments, the behavior expected for $\nu W_2(\nu, q^2) = F_2(x, q^2)$ in theories with anomalous dimensions or in asymptotically

free theories is clear. As $d_0 = 0$ and the d_n's (or A_n's) are monotonically increasing with n, the area under $F_2(x, q^2)$ is constant, while in the region near $x = 1$, probed by large n, $F_2(x, q^2)$ must be falling with q^2. This must be compensated by a rise near $x = 0$, as shown in Fig. 18.

All this can be made quite quantitative in a given field theory by making use of a trick due to Parisi[31], who employed it in the case of anomalous dimensions[32], but it may be applied to asymptotically free theories as well. Consider, for example, the relation between moments at two values of q^2 (both large) in an asymptotically free theory:[33]

$$M_n(q^2) = \left[\frac{\ln(q'^2/\mu^2)}{\ln(q^2/\mu^2)}\right]^{A_n} M_n(q'^2) \quad . \tag{23}$$

Now $M_n(q^2)$ and $M_n(q'^2)$ are the Mellin transforms of $F_2(\omega, q^2)$ and $F_2(\omega, q'^2)$, respectively, while, by definition, $[\ln(q'^2/\mu^2)/\ln(q^2/\mu^2)]^{A_n}$ is the Mellin transform of

$$L\left(\frac{\ln(q'^2/\mu^2)}{\ln(q^2/\mu^2)}, \omega\right) = \frac{1}{2\pi i} \int_{-i\infty}^{+i\infty} ds \left[\frac{\ln(q'^2/\mu^2)}{\ln(q^2/\mu^2)}\right]^{A_s} \frac{1}{\omega^{s+1}} \, , \tag{24}$$

where A_s is the analytic continuation of A_n in the right half complex s plane. Then by the convolution theorem of Mellin transforms one has

$$F_2(\omega, q^2) = \int_1^{\omega} \frac{d\omega''}{\omega''} F_2\left(\frac{\omega}{\omega''}, q'^2\right) L\left(\frac{\ln(q'^2/\mu^2)}{\ln(q^2/\mu^2)}, \omega''\right) \, . \tag{25}$$

Given the structure function for one value of momentum transfer squared $= q'^2$ and for values of the scaling variable between 1 and ω, one can compute it at

another value of q^2 and $2M\nu/q^2 = \omega$, i. e. one has inverted the moments and no longer needs to know the structure function up to infinite ω.

Thus, in an asymptotically free theory, once non-leading terms, presumably of order M^2/q^2, are negligible, and the "effective coupling constant" which behaves as $1/\ln(q^2/\mu^2)$ is small the behavior of $F_2(\omega, q^2)$ from there on is computable, as stressed by Politzer.[34]

An example[35], the case of a structure function whose behavior is governed by only the operators bilinear in quark fields, is shown in Fig. 19. Here the A_n's are taken from a gauge theory with 12 quarks (3 colors × 4 quarks). The structure function has the form $F(x) = 4x^{\frac{1}{2}}(1-x)^3$ at an initial value of the momentum transfer squared, q'^2. The variable

$$s \equiv \ln\left[\frac{\ln(q^2/\mu^2)}{\ln(q'^2/\mu^2)}\right]$$

and if $\mu^2 = 1\ \mathrm{GeV}^2$, $q'^2 = 100\ \mathrm{GeV}^2$, then the curves correspond to $q^2 = 10, 20, 100, 2860$ and $7 \times 10^{18}\ \mathrm{GeV}^2$.

Gross[32] has calculated explicitly the behavior of νW_2 near $\omega = 1$ in a gauge theory with 9 quarks (3 colors × 3 quarks). Assuming the structure function behaves as $(\omega - 1)^d$ near $\omega = 1$, from Eq. (25) it follows in such a theory that[32] for $d = 3$,

$$\frac{F_2(\omega, q^2)}{F_2(\omega, q'^2)} \simeq \left(\frac{\ln(q^2/\mu^2)}{\ln(q'^2/\mu^2)}\right)^{0.69G} \frac{6(\ln\omega')^P}{\Gamma(4+P)} \tag{26}$$

where

$$P = 4G\ln\left[\frac{\ln(q^2/\mu^2)}{\ln(q'^2/\mu^2)}\right]$$

and G is determined from the gauge group and fermion representation to be 4/27 in this case.

A few minutes with a pocket calculator and Eq. (26) produces Fig. 20 for $q'^2/\mu^2 = 5$. Note the large percentage drop in the structure function near threshold. If one chooses the arbitrary scale parameter $\mu^2 = 1\ \mathrm{GeV}^2$, the curves correspond to $q^2 = 5$, 10, 25 and 50 GeV^2, respectively. The qualitative trend of the data available is certainly to drop at fixed ω near 1 with increasing q^2 in this range. Presumably a reasonable value of μ^2 could be found which would fit the experimental observations. Note that the same qualitative behavior of the structure function at fixed ω near 1 is expected in this q^2 range if scaling held in ω'. Thus it is difficult to differentiate at the present time between an approach to true scaling due to non-leading terms, and the deviations from scaling characteristic of the leading term in asymptotically free gauge theories, even though as $q^2 \to \infty$ they are distinctly different.

IV. Other Characteristics of the Leading Singularity

Now let us turn to the other characteristics of the leading light cone singularity in Eq. (10), in view of recent data. With regard to the Lorentz structure we have already noted that in the scaling limit $R = \sigma_L/\sigma_T$ should vanish. A further statement may be made if scaling holds,[39] for then νR should scale.[40,41] It has been known for some time that R is small.[15] In a paper[42] submitted to this conference, and discussed in the parallel session, the MIT-SLAC Spectrometer Facilities Group collaboration shows that $R_n = R_p$ within 0.02 ± 0.03 and that if R_p is fit to a constant, $R_p = 0.16 \pm 0.09$.

Moreover, in their data there is an indication that νR does scale for $\omega \leq 5$, as shown in Fig. 21. For $\omega > 5$ there appears to be a rise of νR with q^2 at fixed ω, although the available data is at low q^2 and this might reflect only a threshold behavior ($R = \sigma_L/\sigma_T$ must vanish at $q^2 = 0$). Restrictions on R in inelastic neutrino scattering[19, 20] may be obtained from several different measured quantities: for example, from $\sigma_T^{\bar{\nu}}/\sigma_T^{\nu}$, where the new Caltech-NAL results[21] demand that $R < 0.3$ averaged over x.

As noted earlier, the SU(3) properties of Eq. (10) provide restrictions on σ_n/σ_p. New information on this is provided by Bodek et al.[43] in a recent experiment done by the MIT-SLAC (SFG) collaboration. The results, with statistical errors only, are shown in Fig. 22. Aside from showing scaling within errors, with increasing values of x the data approach, but do not violate, the lower bound of $\frac{1}{4}$ for σ_n/σ_p. However, the effects of deuterium become increasingly important as $x \to 1$. The ratios shown were corrected from their "raw values" by multiplicative factors of 0.91, 0.74 and 0.40 at x values of 0.73, 0.79, and 0.88 respectively, due to the "smearing" induced by deuterium. While the authors quote reasonable errors for the use of different deuterium wave functions, the off-mass-shell behavior of the struck nucleon, and the use of different parametrizations of the structure functions in the smearing integrals (each $\approx \pm 0.02$ for the last data point in Fig. 22) the large corrections which must be made beyond $x \simeq 0.8$ make me, at least, nervous. It is difficult to be completely confident about quantities like the structure functions for off-mass-shell nucleons. If σ_n/σ_p actually did go to the value of $\frac{1}{4}$ at $x = 1$, or to a value somewhat below or above it, we are very unlikely to establish it by doing electron-deuteron inelastic scattering experiments.

The most spectacular demonstration of the SU(3) structure of Eq. (10) comes from comparing the results of electron and neutrino experiments. Adding the total cross sections for neutrinos and antineutrinos, and assuming $F_2(x) = 2Mx\,F_1(x)$, i.e. $R = 0$, one finds

$$\sigma_{TOT}^{\nu N}(E) + \sigma_{TOT}^{\bar{\nu} N}(E) = \left(\frac{G^2 ME}{\pi}\right)\left(\frac{4}{3}\right)\left[\frac{1}{2}\int_0^1 \left(F_2^{\nu N}(x) + F_2^{\bar{\nu} N}(x)\right) dx\right] \tag{27}$$

With no strange quarks and antiquarks in the nucleon (we will see in a moment that there is only a small integrated antiquark component of any kind), one finds the relation from Eq. (10),

$$\frac{1}{2}\int_0^1 \left(F_2^{\nu N}(x) + F_2^{\bar{\nu} N}(x)\right) dx = \left(\frac{18}{5}\right)\left[\frac{1}{2}\int_0^1 \left(F_2^{ep}(x) + F_2^{en}(x)\right) dx\right]. \tag{28}$$

Thus

$$\frac{5}{18} = \frac{\frac{1}{2}\int_0^1 \left(F_2^{ep}(x) + F_2^{en}(x)\right) dx}{\frac{3\pi}{4G^2 ME}\left[\sigma_{TOT}^{\nu N}(E) + \sigma_{TOT}^{\bar{\nu} N}(E)\right]} . \tag{29}$$

Using the older Gargamelle[19,20] and new Caltech-NAL total cross section data,[21] this relation is tested in Fig. 23, where "Quark Charges" corresponds to the value 5/18 on the left hand side of Eq. (29). Some additional checks on the structure of Eq. (10) involving sum rules have been reported using the Gargamelle data, and are discussed elsewhere.[44]

Even more striking is the simplicity of the matrix elements of the bilocal operators between one nucleon states. Data from Gargamelle[45] at low energies

already indicated the smallness of any antiquark component in the nucleon. The new data supports this strongly. For example, the expected flat y distribution for inelastic neutrino scattering if only quarks are present is compared with the data from the Caltech-NAL experiment[21] in Fig. 24. Similarly, the ratio of total cross sections, $\sigma^{\bar{\nu}N}/\sigma^{\nu N}$, is seen in the two experiments[21,22] at NAL in Figs. 25 and 26, where the value of 1/3 follows if no antiquarks (and no spin zero interacting constituents) are present in the nucleon. The Caltech-NAL experiment puts an upper limit of 10% on the integrated (over x) antiquark component compared to that for quarks.

What antiquark component is seen appears[45,46] to be concentrated at small x ($\lesssim 0.1$). Some caution should be exercised in interpreting even this as evidence for an antiquark component, since in all experiments so far this is a region where the predominant data have low q^2, and where one may not be in the scaling region. Also, up to now all such experiments have been done on complex nuclei, and it is exactly the region of low x (and q^2) where a small component of virtual pions within the nucleus could supply antiquarks off which to scatter. In any case, the smallness of the antiquark component seen now makes it rather clear that Regge pole fits to νW_2 starting at $\omega = 5$ or 10, which then have a large Pomeron contribution (corresponding to quark-antiquark pairs in the nucleon wave function) at these same values of ω, are ruled out. Deep inelastic scattering at $\omega = 10 = 1/x$ does not look like real photon-hadron or hadron-hadron total cross sections at a few GeV, where a few leading Regge singularities, and in particular the Pomeron, already dominate. To a remarkable degree, for $1 < \omega < 10$ the nucleon acts in deep inelastic electron and neutrino scattering as if it were composed of simply three quarks.

V. The Hadronic Final State

Many people hoped, and even predicted, that the hadronic final state in deep inelastic scattering would have a totally different character than in photoproduction or in hadron-hadron collisions. To zeroeth order this has proven not to be the case. But some changes with q^2 have shown up, and may well be connected with the onset of scaling. We will examine just a few examples from data presented to this conference.

1. New data on multiplicities have been presented from a UC Santa Cruz-SLAC collaboration[47] using a muon beam in the streamer chamber at SLAC. While the multiplicity drops $\approx 10\%$ between $q^2 = 0$ and $q^2 \simeq 0.5$ GeV^2, there is no further change out $q^2 \approx 3$ GeV^2. The results for the charged multiplicity at $< q^2 > = 1.36$ GeV^2 versus the total invariant hadronic energy squared, $s = W^2$, are shown in Fig. 27. The values for $< n >$ are shifted down by a roughly constant amount from those in photoproduction, in agreement with earlier results from the DESY[48] streamer chamber and the SLAC bubble chamber,[49] but in disagreement with data from a Cornell experiment.[50] However, all experiments agree that beyond $q^2 \simeq 0.5$ GeV^2 the charged multiplicity depends on the total hadronic energy and not q^2, within errors.

2. Additional information on forward (along the virtual photon's three momentum) inclusive electroproduction of protons comes from the Harvard group[51] working at the Wilson Synchotron at Cornell. As can be seen in Figs. 28 and 29, they find similar invariant inclusive distributions off either a proton or neutron target, which change little with q^2 out to 4 GeV^2 at the same value of W (see Fig. 30). The yield drops rapidly though with increasing W at fixed q^2, as shown in Fig. 31, just as is the case in photoproduction. There seems

little of a "parton character" in these data.

3. Forward pion production, however, shows important changes with q^2. There is some evidence for a change in the slope, b, of the $p_\perp$ distributions (parametrized as $e^{-bp_\perp^2}$), as shown in Fig. 32 from a SLAC experiment,[52] although this is hardly as strong as the $< p_\perp^2 > \propto q^2$ expected in some models.[53] Much more definite and dramatic is a large change in the ratio of forward positive to negative pions. The results from several experiments[47,49,52] are shown in Fig. 33. It is possible that the ratio is both a function of q^2 and of ν in such a way that it depends only on $\omega = 2M\nu/q^2$. This is the prediction of the quark-parton model[12] at sufficiently high ν and q^2 values,[53,54] where the p quark projected forward by the virtual photon should fragment dominantly into π^+'s rather than π^-'s. Data on forward pions produced in inelastic neutrino scattering in Gargamelle, as reported[55] to this conference, in fact agree with the predictions based on the electroproduction data and the quark fragmentation functions extracted therefrom.[56,57,58] This is one place where everything seems to work too well, given the low values of q^2 and ν involved and the experimental difficulties of using complex nuclei as targets.

VI. Other Deep Inelastic Processes Involving Currents

There are a number of related topics which I will not be able to cover here. In particular, papers were submitted on fixed poles in amplitudes involving currents[59], polarized electroproduction,[60] and parton model fits to the structure functions;[61] these are topics which are well reviewed elsewhere.[62] The perennial problem of the lack of shadowing seen in virtual photon-nucleus cross

sections has been reemphasized by a new experimental result from Daresbury,[63] shown in Fig. 34. Attempts at a theoretical understanding of this are to be found in several contributed papers.[64]

The efforts to extend our theoretical success in deep inelastic scattering to other processes involving currents, usually through the parton model, have met with general failure up to this point. Some all too familiar examples are:

1. Electron-Positron Annihilation into Hadrons.

We have heard from Professor Richter[65] about out theoretical lack of success in understanding e^+e^- annihilation. Here I would like to concentrate on a much more limited question, that of "crossing" from the space-like to time-like region near $\omega = 1$. For certain classes of graphs the structure functions in the two regions are analytic continuations of one another, as in the model of Drell, Levy and Yan.[66] An analysis of field theoretic models, as carried out by Landshoff and Polkinghorne,[67] shows that this is not true in general, the trouble being traceable to certain "double discontinuity" terms.[67]

However, Gatto et al.[68] have shown for a large class of graphs in field theory that if we define $\bar{\omega} = -2p\cdot q/q^2 = \omega$, there is a connection at the point $\bar{\omega} = 1 = \omega$, where the domains of, say, $e^+e^- \to \bar{p}$ + anything $(0 \leq \bar{\omega} \leq 1)$ and $ep \to e$ + anything, $(1 \leq \omega \leq \infty)$ touch. More precisely, if $\bar{F}(\bar{\omega}) = c_1(1-\bar{\omega})^{p_1}$ as $\bar{\omega} \to 1^-$ in e^+e^- annihilation and $F(\omega) = c_2(\omega-1)^{p_1}$ as $\omega \to 1^+$ in electroproduction, then $c_1 = c_2$ and $p_1 = p_2$. This result follows as a particular case of the formula of Gribov and Lipatov:[69]

$$\bar{\omega}\,\bar{F}_1(\bar{\omega}) = F_1(1/\bar{\omega} = \omega) \quad , \qquad \bar{\omega}^3\,\bar{F}_2(\bar{\omega}) = F_2(1/\bar{\omega} = \omega) \tag{30}$$

derived by summing graphs in a particular field theory model.[70]

As a first step toward an examination of this experimentally, let us assume F_1 and F_2 for $ep \to e$ + anything are related by $F_2 = (2M/\omega)F_1$, i.e. $\sigma_L/\sigma_T = 0$, and that correspondingly $\overline{F}_2(\overline{\omega}) = (2M/\overline{\omega})\overline{F}_1(\overline{\omega})$. In the relativistic limit, one finds then that

$$\frac{\overline{\omega}}{\sigma_{\mu\mu}} \frac{d\sigma}{d\overline{\omega}} = \overline{\omega}^3 \overline{F}_2(\overline{\omega}) , \tag{31}$$

where the right hand side is also equal to $F_2(1/\overline{\omega} = \omega)$ according to Gribov and Lipatov.[69]

A number of precautionary statements are in order before examining the comparison with SPEAR data[65, 71] on $\overline{p}$ production: (a) the $\overline{p}$'s are characterized by mean momenta of ≈ 0.5 GeV, so the relativistic result in Eq. (31) doesn't hold, although this has effects which would both raise and lower the true value of $\overline{\omega}^3 \overline{F}_2(\overline{\omega})$, compared to $(\overline{\omega}\, d\sigma/d\overline{\omega})/\sigma_{\mu\mu}$. (b) Some $\overline{\Lambda}$'s are known to be produced and will contaminate the $\overline{p}$ sample on decaying. (c) The errors shown are statistical only. The overall cross sections are not known to better than 20%, which does not include any error from my extracting cross section from various graphs. The whole exercise should only be trusted to a factor of two.

With those caveats, the comparison of $(\overline{\omega}\, d\sigma/d\overline{\omega})/\sigma_{\mu\mu}$ for $e^+e^- \to \overline{p}$ + anything with $F_2(\omega = 1/\overline{\omega})$ for $ep \to e$ + anything is made in Fig. 35, where the dashed line is the "reflection" of the $ep \to e$ + anything data and corresponds to the prediction of Eq. (30). The agreement, even as to order of magnitude is surprising to me. However, before we rejoice, even more surprising is the result of taking pion production at SPEAR at $\overline{\omega} = 0.5$ (where the pion $\overline{\omega}$

distribution may well scale) and doing the reverse — predicting $F^{e\pi}(\omega = 2)$. The result is an order of magnitude larger than that measured for $F^{ep}(\omega = 2)$. This would violate at least parton model sum rules, and more importantly, one's intuition, if it were true over a range of ω values.[72] We still have our most pressing failure in understanding e^+e^- annihilation.

2. $pp \to \mu^+\mu^- +$ Anything.

This process was first discussed in the parton model by Drell and Yan[73] where it has its origins in parton-antiparton annihilation and there is a resulting scaling law of the form

$$\frac{d\sigma}{dQ^2} = \frac{4\pi\alpha^2}{3Q^4} f(Q^2/s) , \tag{32}$$

where Q^2 is the invariant mass squared of the lepton pair and s the total center of mass energy squared. Recently a number of authors[74] have reconsidered this process in the light of the electron and neutrino data which shows an absence of antiquark partons. In particular, Einhorn and Savit[74] have employed a general technique of deriving bounds in situations with inequality constraints, and applied it using the electron and neutrino data to obtain the upper bound on the Drell-Yan contribution shown as the solid line in Fig. 36. The data (dashed line) is from the experiment of Christensen et al.[75] at Brookhaven. It is fairly clear that the theory doesn't have much to say in regard to the cross section observed in this experiment.

3. Inelastic Compton Scattering.

The process $\gamma + p \to \gamma +$ anything was suggested by Bjorken and Paschos[13] as a possible test of the parton model. They predicted the simple relation

$$\left(\frac{d\sigma}{d\Omega dE'}\right)_{\gamma p} = \frac{(E-E')^2}{EE'} \frac{\langle \sum_i Q_i^4 \rangle}{\langle \sum_i Q_i^2 \rangle} \left(\frac{d\sigma}{d\Omega dE'}\right)_{ep}, \tag{33}$$

between the inelastic Compton and inelastic electron scattering cross sections, where Q_i is the charge (in units of e) of the i'th parton. In a paper[76] submitted to this conference by a UC Santa Barbara group working with a 21 GeV bremsstrahlung beam at SLAC, the results of such an inelastic Compton scattering experiment are reported. After subtracting off photons coming from π^0's and η^0's (which turn out to have $\approx \frac{1}{2}$ the yield of π^0's), they are left with an excess of single photons, shown in Fig. 37. The solid line is the averaged single γ yields that result,while the dashed line is the Bjorken-Paschos prediction for charge one partons, i.e. $< \sum Q_i^4 > = < \sum Q_i^2 >$. Especially at the highest $p_\perp$ values it seems the yields lie significantly above even the charge-one parton model predictions.[77] The parton model doesn't appear to have much to do with this data either.

VII. Conclusion

We find ourselves in a somewhat puzzling situation. On the one hand the world is far simpler than we had any right to expect. Not only do all the characteristics of the quark light cone algebra or the quark parton model as applied to deep inelastic scattering seem to be borne out when compared with experiment, but to a very good approximation the nucleon acts as if composed of only quarks, and not antiquarks.

On the other hand, our attempts to extend parton ideas to other processes involving currents has not met with any clear success, and the present situation is far more complicated than we had every right to hope. The comparison of the parton model with e^+e^- annihilation, $pp \to \mu^+\mu^-$ + anything, and $\gamma p \to \gamma$ + anything data is at best inconclusive and at worst dismal.

As for scaling itself in deep inelastic scattering, what we see is certainly consistent with rather small anomalous dimensions, although that holds no beauty for me. A more desirable alternative lies in the asymptotically free gauge theories, where scaling is only broken logarithmically, and which are perhaps even suggested by some of the new data we have reviewed. However, true Bjorken scaling is hardly ruled out. Further precision measurements near $\omega = 1$ at the highest q^2 possible are of central importance in examining which alternative is currect. For a decisive exploration of the large ω (≈ 100) and q^2 (10-50 GeV^2) regime we must await electron-proton colliding beams. But my general feeling on the subject of this talk, including scaling, is perhaps best summarized in a question: who would have thought six years ago in Vienna that the data presented there, plus the idea of three point quarks in the nucleon, would permit one to predict to within 20% or better the results of the electron, muon, neutrino and antineutrino deep inelastic scattering experiments performed since then, which now extend over almost two orders of magnitude in ν and q^2?

Acknowledgement

My thanks to the scientific secretaries, Drs. P. R. Norton and R. L. Heimann, and to the parallel session organizers, Professors H. Meyer and B. C. Barish, for much help and many discussions.

References

1. W. K. H. Panofsky, rapporteur's talk in Proceedings of the Fourteenth International Conference on High Energy Physics, Vienna, Austria (CERN Scientific Information Service, Geneva, Switzerland, 1968), p. 23.
2. J. D. Bjorken, Phys. Rev. 179, 1547 (1969).
3. J. S. Poucher et al., Phys. Rev. Letters 32, 118 (1974).
4. The kinematics of inelastic scattering are reviewed in F. J. Gilman, Phys. Reports 4C, 98 (1972). See references to other work therein.
5. For a review of the subject of light cone and short distance singularities, see Y. Frishman, in Proceedings of the XVI International Conference on High Energy Physics, J. D. Jackson and A. Roberts, editors (National Accelerator Laboratory, Batavia, Illinois, 1972), p. 119. See references to previous work therein. I thank Professor Frishman for his comments on this part of the talk.
6. K. Wilson, Phys. Rev. 179, 1499 (1969).
7. We have been somewhat schematic in writing Eq. (4). If other operators contribute to the same order, with say different isospin or SU(3) properties, then one must add an additional summation index (see Ref. 5).
8. D. J. Gross and F. Wilczek, Phys. Rev. Letters 30, 1343 (1973); G. 't Hooft (unpublished); H. D. Politzer, Phys. Rev. Letters 30, 1346 (1973).
9. S. Coleman and D. J. Gross, Phys. Rev. Letters 31, 851 (1973). D. J. Gross and F. Wilczek, Phys. Rev. D8, 3633 (1973) and D9, 980 (1974); H. Georgi and H. D. Politzer, Phys. Rev. D9, 416 (1974).
10. H. Fritzsch and M. Gell-Mann, in Scale Invariance and the Light Cone (Gordon and Breach, New York, 1971), Vol. 2, p. 1.

11. O. Nachtmann, Nucl. Phys. B38, 397 (1972).

12. R. P. Feynman, Phys. Rev. Letters 23, 1415 (1969); and R. P. Feynman, Photon-Hadron Interactions (W. A. Benjamin, Reading, Mass., 1972).

13. J. D. Bjorken and E. A. Paschos, Phys. Rev. 185, 1975 (1969).

14. A. Bodek et al., SLAC preprint SLAC-PUB-1442, 1974 (unpublished), and paper No. 765, submitted to this conference. See parallel session.

15. G. Miller et al., Phys. Rev. D5, 528 (1972). See also E. D. Bloom et al., SLAC-PUB-796, report presented to the XV International Conference on High Energy Physics, Kiev, 1970 (unpublished).

16. W. B. Atwood et al., papers No. 895 and 896 submitted to this conference. See parallel session.

17. For example, see J. C. Pati and A. Salam, Phys. Rev. Letters 32, 1083 (1974). See also E. D. Bloom, talk at the Trieste Conference, June,1974 (unpublished) and B. Richter, rapporteur's talk, these proceedings.

18. D. J. Fox et al., paper No. 330 submitted to this conference. See parallel session.

19. D. H. Perkins, in Proceedings of the XVI International Conference on High Energy Physics, J. D. Jackson and A. Roberts, editors (National Accelerator Laboratory, Batavia, 1972), Vol. 4, p. 189.

20. D. Cundy, rapporteur's talk, these proceedings.

21. B. C. Barish et al., papers No. 586 and 588 submitted to this conference. See parallel session.

22. B. Aubert et al., papers No. 691 and 694 submitted to this conference. See parallel session.

23. M. Chanowitz and S. D. Drell, Phys. Rev. Letters 30, 807 (1973) and Phys. Rev. D9, 2078 (1974).

24. G. B. West, Stanford University preprint, 1974 (unpublished). See also K. Matumoto and T. Tajima, paper No. 156 submitted to this conference and V. Barger, Phys. Letters 49B, 43 (1974) and paper No. 173 submitted to this conference.

25. G. B. West and P. Zerwas, SLAC and Stanford preprint, SLAC-PUB-1420, ITP-465, 1974 (unpublished).

26. See also E. W. Colglazier and R. Rajaraman, Institute for Advance Study preprint, 1974 (unpublished).

27. J. C. Polkinghorne, parallel session, these proceedings.

28. See also the recent analysis of precocious scaling and duality of M. B. Einhorn and G. C. Fox, NAL preprint, FNAL-Pub-74/57-THY, 1974 (unpublished).

29. E. D. Bloom, invited talk at the Bonn conference, 1973 and SLAC-PUB-1319, 1973 (unpublished).

30. O. Nachtmann, Vienna preprint, 1974 (unpublished).

31. G. Parisi, Phys. Letters 43B, 207 (1973), and Columbia University preprint, 1974 (unpublished).

32. See also Y. Frishman, in Proceedings of the Summer Institute on Particle Physics, July 9-28, 1973, SLAC Report No. 167, Vol. I, p. 93 (1973).

33. D. J. Gross, Phys. Rev. Letters 32, 1071 (1974). See parallel session. Near $\omega = 1$ the behavior of the structure function is presumably governed by the operators constructed from the fermion fields, with computable A_n's.

34. H. D. Politzer, Phys. Rev. D9, 2174 (1974). See also H. Fritzsch and P. Minkowski, Caltech preprints, 1974 (unpublished).

35. A. De Rujula, H. Georgi, and H. D. Politzer, Harvard preprint, 1974 (unpublished). See parallel session. See also Ref. 31.

36. D. J. Gross and S. B. Treiman, Phys. Rev. Letters 32, 1145 (1974).

37. A. De Rujula, Phys. Rev. Letters 32, 1143 (1974).

38. A. De Rujula et al., Harvard and Princeton preprint, 1974 (unpublished). See also S. J. Orfanidis and V. Rittenberg, Rockefeller preprint, 1974 (unpublished).

39. In asymptotically free theories $R = \sigma_L/\sigma_T$ vanishes as $1/\ln(q^2/\mu^2)$. See Refs. 8 and 9.

40. K. T. Mahanthappa and T. Yao, Phys. Letters 39B, 549 (1972); J. E. Mandula, Phys. Rev. D8, 328 (1973).

41. See also R. L. Heimann, Cambridge preprint, 1974 (unpublished) and paper No. 189 submitted to this conference.

42. E. M. Riordan et al., SLAC preprint SLAC-PUB-1417, 1974 (unpublished) and paper No. 762 submitted to this conference. See parallel session.

43. A. Bodek et al., SLAC preprint SLAC-PUB-1399, 1974 (unpublished), and paper No. 763 submitted to this conference. See parallel session.

44. H. Deden et al., paper No. 512 submitted to this conference. See D. Cundy, Ref. 20 for a discussion of these results.

45. See papers No. 511, 512, and 513 submitted to this conference by the Gargamelle Neutrino Collaboration and the reviews of D. Perkins, Ref. 19, and D. Cundy, Ref. 20.

46. B. C. Barish, private communication.

47. K. Bunnell et al., papers No. 207, 208, and 209 submitted to this conference. See parallel session.

48. V. Eckardt et al., paper No. 392 submitted to this conference.

49. See J. T. Carroll in Proceedings of the Summer Institute on Particle Physics, July 9-28, 1973, SLAC Report No. 167, Vol. I, p. 157 (1973); and J. Ballam et al., paper submitted to the Bonn Conference, 1973 (unpublished).

50. P. H. Garbincius et al., Phys. Rev. Letters 32, 328 (1974); A. J. Sadoff et al., Phys. Rev. Letters 32, 955 (1974); B. Gibbard et al., Cornell preprint CLNS-266, 1974 (unpublished).

51. C. J. Bebek et al., paper No. 573 submitted to this conference. See parallel session.

52. J. T. Dakin et al., SLAC preprint SLAC-PUB-1421, 1974 (unpublished) and paper No. 160 submitted to this conference. See parallel session and also C. J. Bebek et al., paper No. 575 submitted to this conference.

53. The status of models for hadron production by leptons is reviewed by F. J. Gilman, invited talk at the Irvine Conference, December, 1973, and SLAC-PUB-1396, 1974 (unpublished). See references to earlier works therein.

54. See the discussion of the theory by R. N. Cahn in the parallel session, these proceedings.

55. See the discussion of the data by D. Cundy, rapporteur's talk, these proceedings.

56. J. T. Dakin and G. J. Feldman, Phys. Rev. D8, 2862 (1973). See also P. Hasenfratz, Phys. Letters 47B, 60 (1973).

57. C. H. Albright and J. Cleymans, CERN preprint TH.1829, 1974 (unpublished).

58. In a related theoretical contribution, J. D. Stack, paper No. 397 submitted to this conference, argues that field theories with anomalous dimensions which approach constants as $n \to \infty$ (e.g. parton models with scaling) would

have jets in the final state, whereas theories where the anomalous dimensions grow with n without limit (including asymptotically free theories) need not have jet structure.

59. H. Goldberg, paper No. 170 submitted to this conference; C. A. Dominguez and H. Moreno, paper No. 279 submitted to this conference; R. P. Worden, paper No. 635 submitted to this conference.

60. F. E. Close, paper No. 261 submitted to this conference; A. Le Yaouanc et al., paper No. 416 submitted to this conference; R. L. Heimann, paper No. 766 submitted to this conference.

61. V. Barger and R. J. N. Phillips, paper No. 174 submitted to this conference; R. McElhaney and S. F. Tuan, paper No. 241 submitted to this conference.

62. See, for example, F. J. Gilman in Proceedings of the Summer Institute on Particle Physics, July 9-28, 1973, SLAC Report No. 167, Vol. I, pps. 71 and 82 (1973).

63. J. Bailey et al., paper No. 295 submitted to this conference.

64. See the recent work of M. Greco and Y. N. Srivastava, Frascati preprint LNF-74/3(p), 1974 (unpublished); G. Cocho et al., Trieste preprint IC/73/171, 1973 (unpublished); and also H. Fraas, B. Read, D. Schildknecht, paper No. 550 submitted to this conference; N. N. Nikolaev and V. I. Zakharov, paper No. 858 submitted to this conference.

65. B. Richter, rapporteur's talk, these proceedings.

66. S. D. Drell, D. J. Levy, and T. M. Yan, Phys. Rev. D1, 1617 (1970).

67. P. V. Landshoff and J. C. Polkinghorne, Nucl. Phys. B53, 473 (1973); and H. D. Dahmen and F. Steiner, Phys. Letters 43B, 217 (1973); R. Gatto and I. Vendramin, Rome preprint INFN-Rome-482 (1973) (unpublished).

68. R. Gatto, P. Menotti, and I. Vendramin, Nuovo Cimento Letters 5, 754 (1972), and Phys. Rev. D7, 2524 (1973); see also Landshoff and Polkinghorne, Ref. 67.

69. V. N. Gribov and L. N. Lipatov, Yad. Fiz. 15, 1218 (1972) [Sov. J. Nucl. Phys. 15, 675 (1972)]. See also the recent model of G. Schierholz and M. G. Schmidt, Phys. Letters 48B, 341 (1974) and Phys. Rev., in press.

70. See the review of J. Sullivan, in Proceedings of the Summer Institute on Particle Physics, July 9-28, 1973, SLAC Report 167, Vol. I, p. 289 (1973).

71. C. Morehouse, private communication.

72. Y. Eylon and Y. Zarmi, Weizmann Institute preprint WIS-74/31, 1974 (unpublished) have recently examined in detail the possible equality between the distribution of a hadron in a parton's fragmentation and of the parton inside the hadron. Within the parton model this leads directly to the Gribov-Lipatov relation.

73. S. D. Drell and T. M. Yan, Phys. Rev. Letters 25, 316 (1970) and Ann. Phys. (N.Y.) 66, 578 (1971).

74. M. B. Einhorn and R. Savit, NAL preprints NAL-Pub-74/35-THY and NAL-Pub-74/41-THY, 1974 (unpublished); G. R. Farrar, Caltech preprint CALT-68-422-A, 1974 (unpublished); S. Pakvasa, D. Parashar, and S. F. Tuan, paper No. 242 submitted to this conference; H. Paar and M. Paschos, NAL preprint NAL-Pub-74/29-THY, 1974 (unpublished).

75. J. H. Christenson et al., Phys. Rev. D8, 2016 (1973).

76. D. O. Caldwell et al., paper No. 302 submitted to this conference. See parallel session.

77. An earlier Cornell experiment on photoproduction of low mass muon pairs also reported a large excess over the expected yield from Bethe Heitler and inelastic Compton processes. See J. F. Davis et al., Phys. Rev. Letters 29, 1356 (1972). Preliminary results from the measurement of the difference between $e^+ + p \rightarrow e^+ + \gamma$ + anything and $e^- + p \rightarrow e^- + \gamma$ + anything, which could arise from the interference of Bethe-Heitler and virtual Compton amplitudes, also indicates an excess over parton model predictions — D. O. Caldwell et al., paper No. 303 submitted to this conference and private communication.

Figure Captions

Fig. 1 — Inelastic electron-proton scattering data for $\theta = 6^{o}$, as presented at the Vienna conference.[1]

Fig. 2 — The structure function νW_2 for $\theta = 6^{o}$ and 10° inelastic scattering on hydrogen and deuterium.[3]

Fig. 3 — The structure functions νW_2 and $2MW_1$ at various fixed values of ω, plotted[14] versus q^2.

Fig. 4 — The structure functions νW_2 and $2MW_1$ for various q^2 ranges, plotted[15] versus ω'.

Fig. 5 — Comparison of 13.9 GeV positron-proton and electron-proton inelastic scattering.[16]

Fig. 6 — Configurations of the apparatus of Ref. 18 at 56.3 and 150 GeV for the direct test of scaling.

Fig. 7 — Results of the comparison of 56 GeV with 150 GeV data versus q^2 and of each energy separately with a Monte Carlo simulation of the experiment.[18] Figures (a), (b), (c), (d) show the observed q^2 distribution under various cuts on the beam; (e) is the detection efficiency versus q^2; (f) is the ratio comparison of 150 GeV data/56 GeV data; (g) is the ratio of 150 GeV data to a Monte Carlo calculation based on a fit to SLAC data; (h) is the same, but for $\omega < 9$; and (j) is the ratio of 56 GeV data to a Monte Carlo calculation based on a fit to SLAC data. All errors shown are statistical only.

Fig. 8 — Effects of various types of systematic errors and the radiative correction on the direct test of scaling of Ref. 18.

Fig. 9 — Neutrino and antineutrino total cross sections at $< E >$ values of 38 and 108 GeV from Ref. 21.

Fig. 10 — Neutrino-nucleon total cross sections from Ref. 22.

Fig. 11 — Antineutrino-nucleon total cross sections from Ref. 22.

Fig. 12 — $< Q^2 >$ versus incident energy, E, for neutrinos.[22]

Fig. 13 — $< Q^2 >$ versus incident energy, E, for antineutrinos.[22]

Fig. 14 — Q^2 distribution for neutrino events from Ref. 21 compared with expectation based on $F_2^{ed}(x)$ from SLAC.

Fig. 15 - Comparison of the x distribution for neutrinos of Ref. 21 with expectation based on $F_2^{ed}(x)$ from SLAC.

Fig. 16 — Comparison of the x distribution for neutrinos and antineutrinos from Ref. 22 with expectation based on SLAC measurements of structure functions in inelastic electron scattering.

Fig. 17 — Deviations[25] of the total cross sections for neutrinos and antineutrinos from linearity in E due to non-zero values of the quark magnetic moment and $1/\Lambda^2$.

Fig. 18 — Expected form of the change in $F_2(\omega, q^2)$ in theories with anomalous dimensions and in asymptotically free gauge theories for increasing q^2: $q_2^2 > q_1^2$.

Fig. 19 — Change with q^2 of a structure function whose behavior is governed only by operators bilinear in quark fields in an asymptotically free gauge theory[35] (see text).

Fig. 20 — Change with q^2 of the structure function $F_2(\omega, q^2)$ near $\omega = 1$ in an asymptotically free theory.[32]

Fig. 21 — νR at various fixed values of ω as a function of q^2 from Ref. 42.

Fig. 22 — Ratio[43] of inelastic electron-neutron to electron-proton inelastic scattering versus $x = 1/\omega$ and $x' = 1/\omega'$.

Fig. 23 — Comparison[21] of the ratio of integrated electron-nucleon to neutrino-nucleon structure functions to the value of 5/18 expected from "Quark Charges."

Fig. 24 — Comparison[21] of the y distribution in neutrino-nucleon inelastic scattering to a Monte Carlo calculation based on the flat distribution expected if only quarks are present in the nucleon.

Fig. 25 — Ratio of antineutrino to neutrino total cross sections from Ref. 21.

Fig. 26 — Ratio of antineutrino to neutrino total cross sections from Ref. 22.

Fig. 27 — Charged hadron multiplicity as a function of $s = W^2$ in inelastic electron-proton scattering.

Fig. 28 — Invariant inclusive distribution,[51] $(E\, d^3\sigma/dp^3)/\sigma_T$, for forward proton production by a virtual photon with $q^2 = 1.19\ \mathrm{GeV}^2$ on a proton target.

The photon-nucleon system has total center of mass energy $W = 2.21$ GeV. $x' = p_L / \left[p_{max}^2 - p_\perp^2\right]^{\frac{1}{2}}$, and for the data here, $p_\perp^2 < 0.02$ GeV^2.

Fig. 29 — Same[51] as Fig. 28, but a neutron target.

Fig. 30 — Same[51] as Fig. 28, but at $q^2 = 3.92$ GeV^2.

Fig. 31 — Same[51] as Fig. 28, but at $W = 3.04$ GeV.

Fig. 32 — Slope, b, of the $p_\perp^2$ distribution[52] for forward pion production as a function of q^2.

Fig. 33 — Ratio of positive to negative forward-going hadrons in electroproduction off protons as a function of q^2.

Fig. 34 — Dependence[63] on atomic number, A, of the virtual photon-nucleus total cross section at $q^2 = 0.12$ and 0.25 GeV^2, and in photoproduction ($q^2 = 0$).

Fig. 35 — Values[65, 71] of $(\bar{\omega}\, d\sigma/d\bar{\omega})/\sigma_{\mu\mu}$ for $e^+e^- \to \bar{p}$ + anything compared to values[3] of $F_2(\omega')$ for $ep \to e$ + anything. The solid line is a fit[15] to the electroproduction data, and its "reflection," the dashed line, is what is expected from Eq. (30) (see text).

Fig. 36 — Upper bound[74] (solid line) on the Drell-Yan contribution to $pp \to \mu^+\mu^-$ + anything compared to the data[75] (dashed line) as a function of $\tau = Q^2/s$.

Fig. 37 — Comparison[76] of the "single photon excess" yields (solid lines) for $\gamma + p \rightarrow \gamma +$ anything at $p_\perp = 1.1$, 1.3, 1.5, and 1.7 GeV/c in (a), (b), (c), and (d) respectively, with the charge-one parton prediction[13] (dashed line). See text.

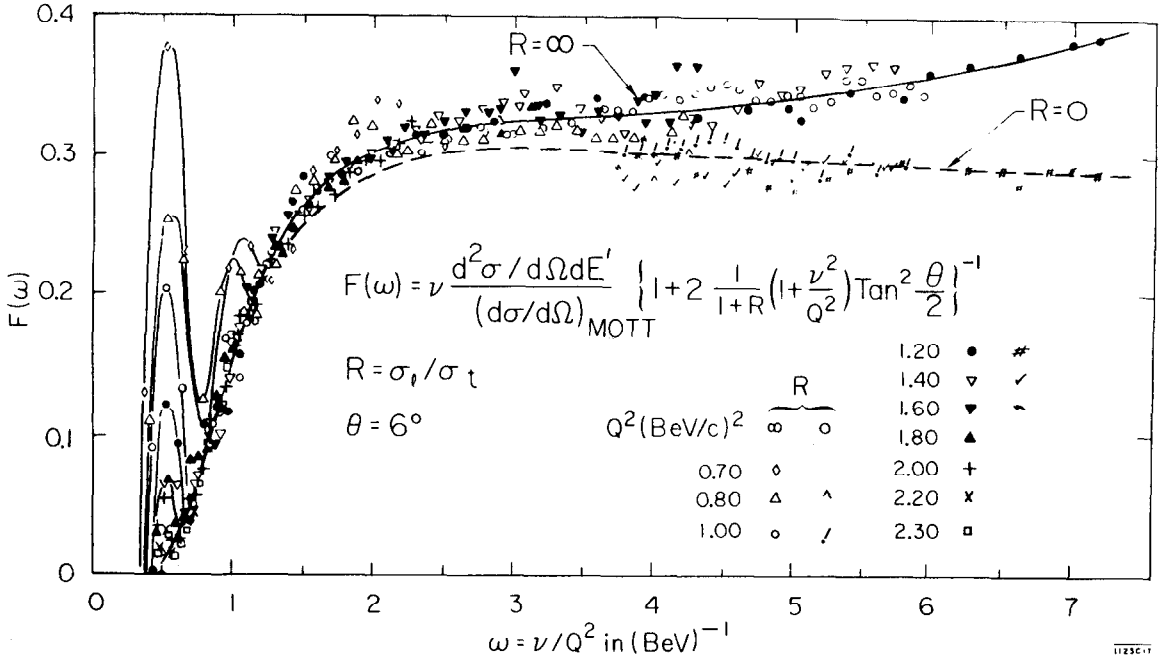
0.4
0.3
0.2
0.1
0
F(ω)
R=∞
R=0
$F(\omega) = \nu \frac{d^2\sigma / d\Omega dE'}{(d\sigma/d\Omega)_{MOTT}} \left\{ 1 + 2 \frac{1}{1+R} \left(1 + \frac{\nu^2}{Q^2}\right) \mathrm{Tan}^2 \frac{\theta}{2} \right\}^{-1}$
$R = \sigma_l / \sigma_t$
$\theta = 6°$
R
Q^2(BeV/c)^2
∞
0
0.70
0.80
1.00
1.20
1.40
1.60
1.80
2.00
2.20
2.30
0
1
2
3
4
5
6
7
$\omega = \nu / Q^2$ in (BeV)$^{-1}$

Fig. 1

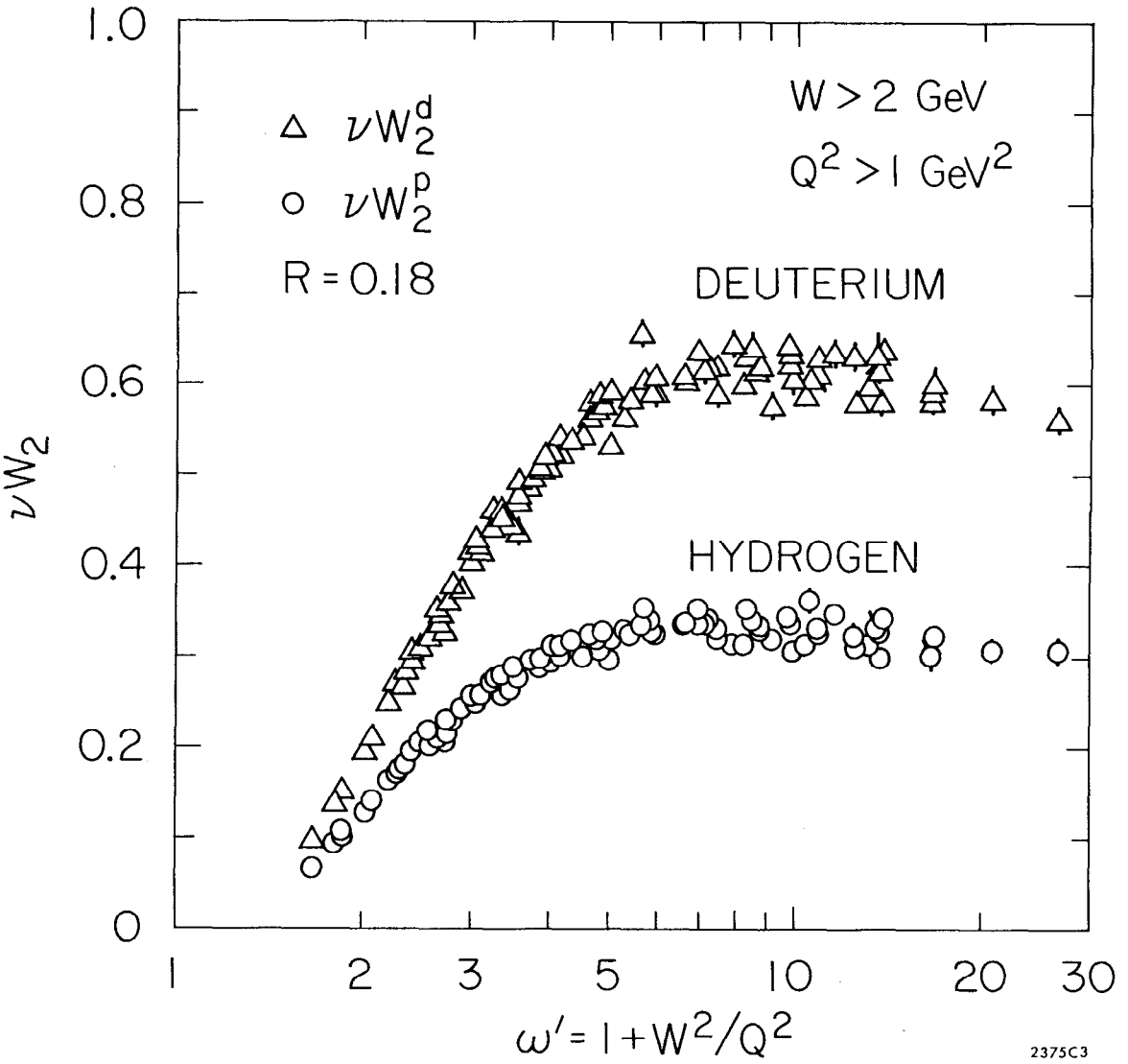
1.0
0.8
0.6
0.4
0.2
0
νW_2
νW_2^d
νW_2^p
R = 0.18
W > 2 GeV
$Q^2 > 1$ GeV^2
DEUTERIUM
HYDROGEN
1
2
3
5
10
20
30
$\omega' = 1 + W^2/Q^2$
2375C3

Fig. 2

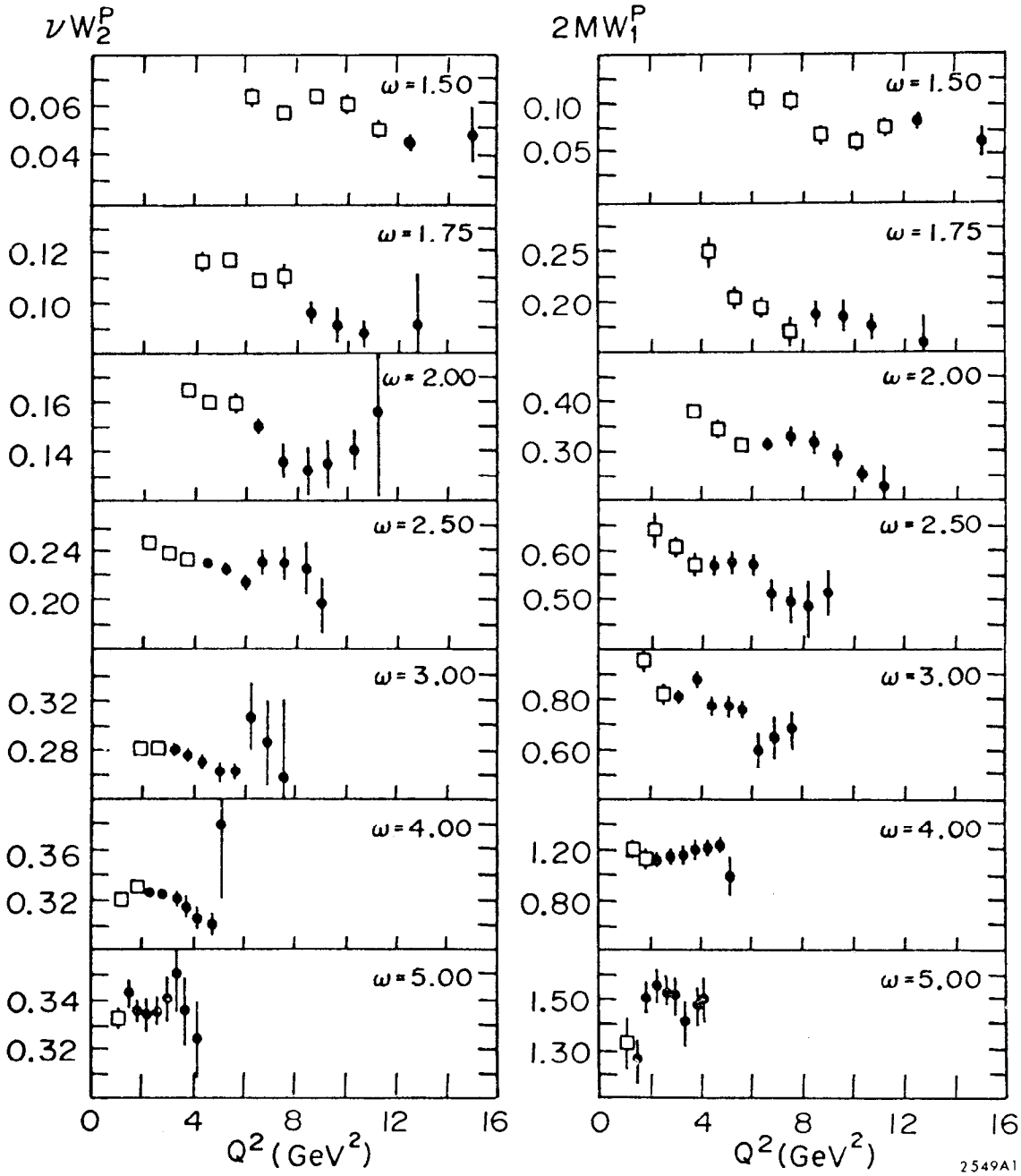
νW_2^P
$2MW_1^P$
ω = 1.50
ω = 1.75
ω = 2.00
ω = 2.50
ω = 3.00
ω = 4.00
ω = 5.00
0.06
0.04
0.12
0.10
0.16
0.14
0.24
0.20
0.32
0.28
0.36
0.32
0.34
0.32
0.10
0.05
0.25
0.20
0.40
0.30
0.60
0.50
0.80
0.60
1.20
0.80
1.50
1.30
0
4
8
12
16
Q^2 (GeV^2)
2549A1

Fig. 3

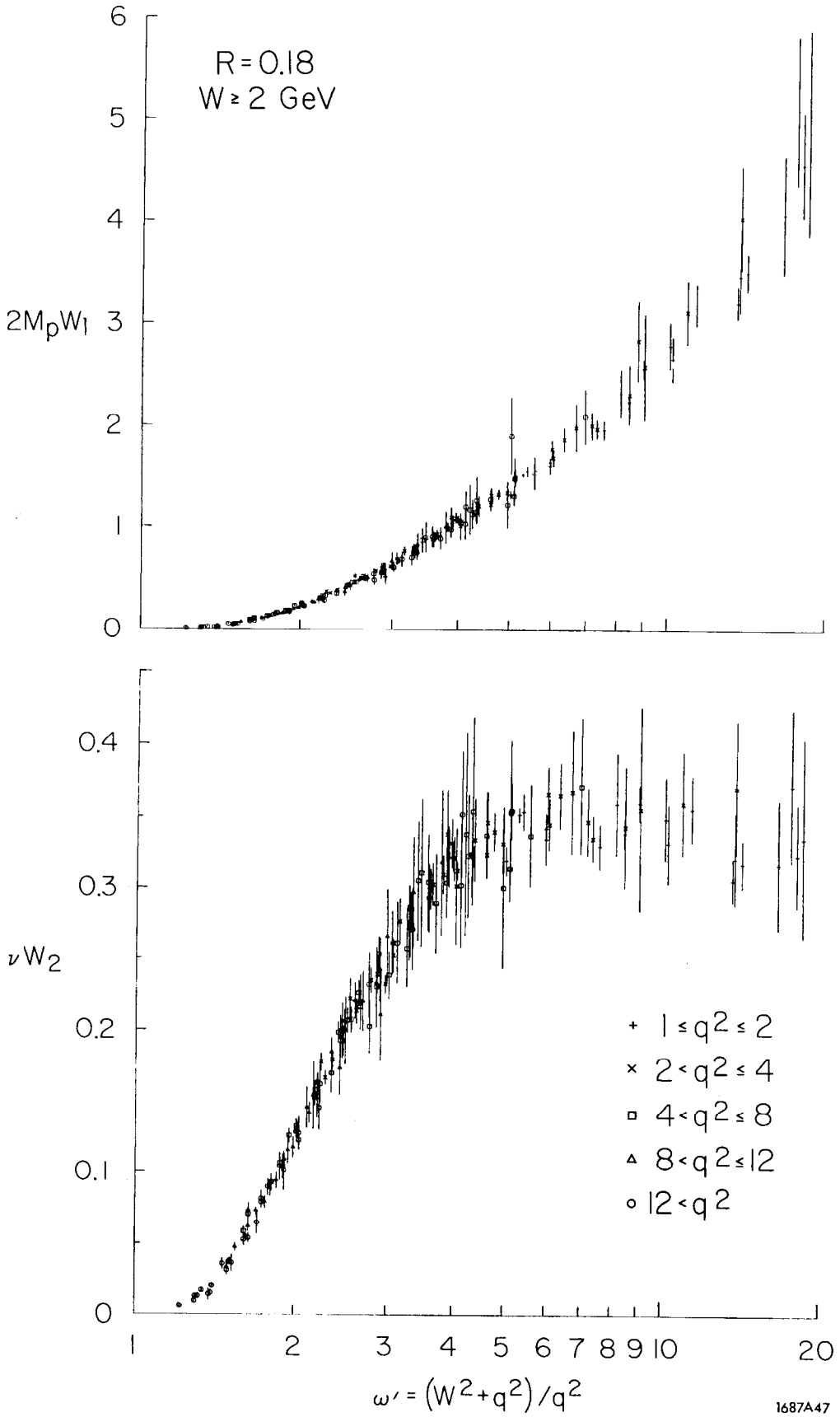
R = 0.18
W ≥ 2 GeV
$2M_pW_1$
νW_2
+ $1 \le q^2 \le 2$
× $2 < q^2 \le 4$
□ $4 < q^2 \le 8$
△ $8 < q^2 \le 12$
○ $12 < q^2$
$\omega' = (W^2+q^2)/q^2$
1687A47

Fig. 4

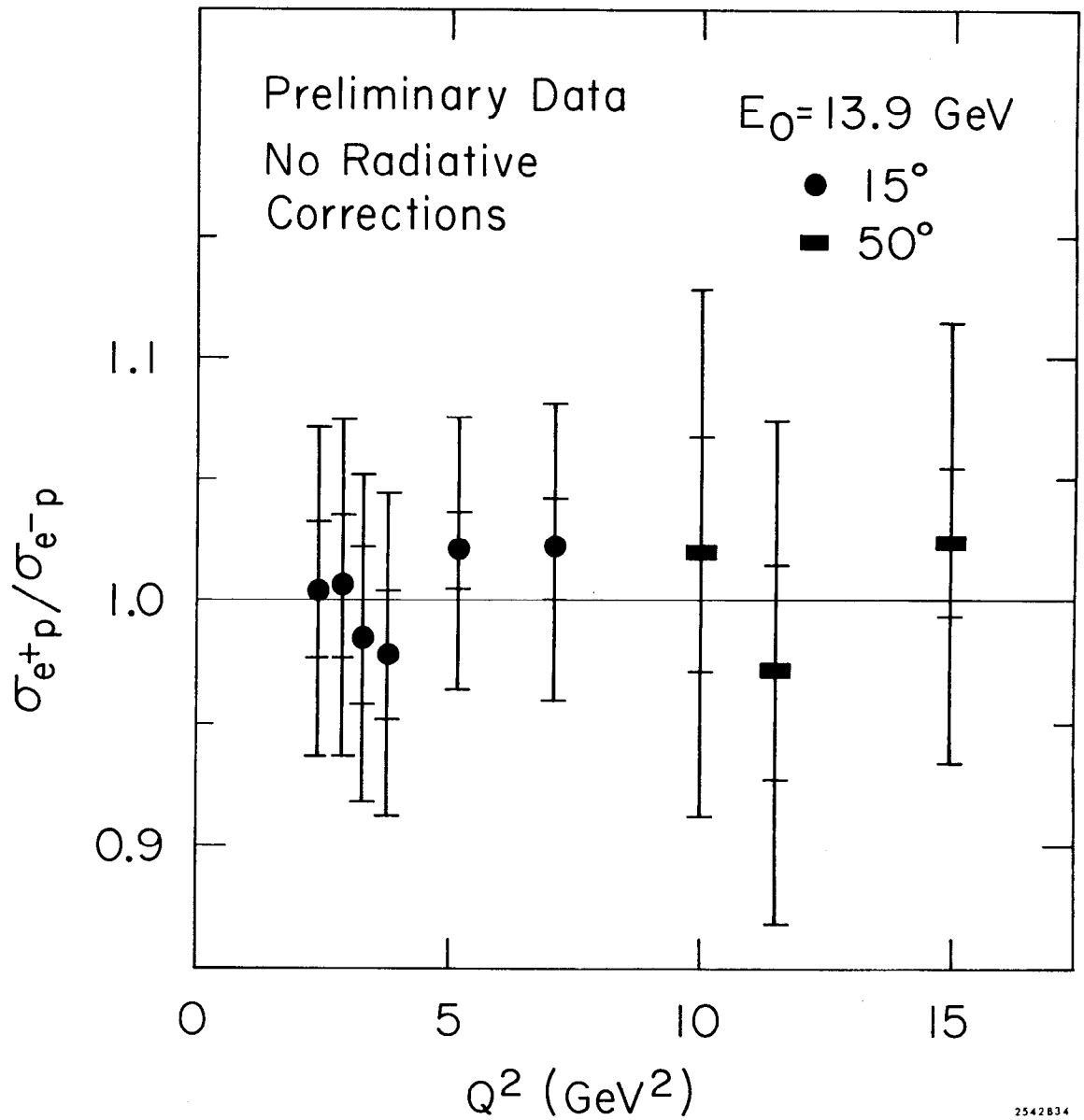
Preliminary Data
No Radiative
Corrections
E_0= 13.9 GeV
15°
50°
1.1
1.0
0.9
$\sigma_{e^+p}/\sigma_{e^-p}$
0
5
10
15
Q^2 (GeV^2)
2542B34

Fig. 5

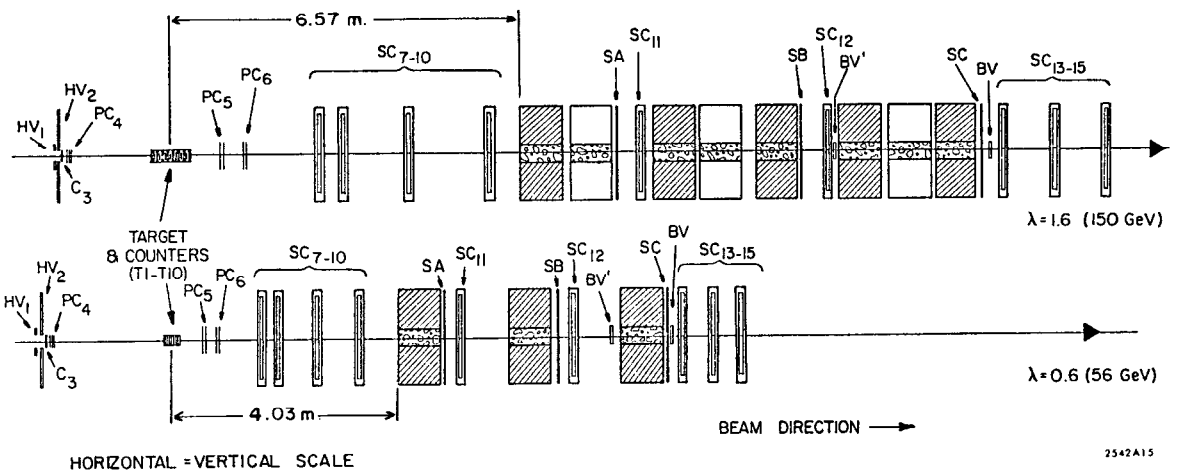
6.57 m.
HV1
HV2
PC4
C3
PC5
PC6
SC7-10
SA
SC11
SB
SC12
BV'
SC
BV
SC13-15
λ=1.6 (150 GeV)
TARGET
& COUNTERS
(T1-T10)
4.03 m
λ=0.6 (56 GeV)
BEAM DIRECTION
HORIZONTAL = VERTICAL SCALE
2542A15

Fig. 6

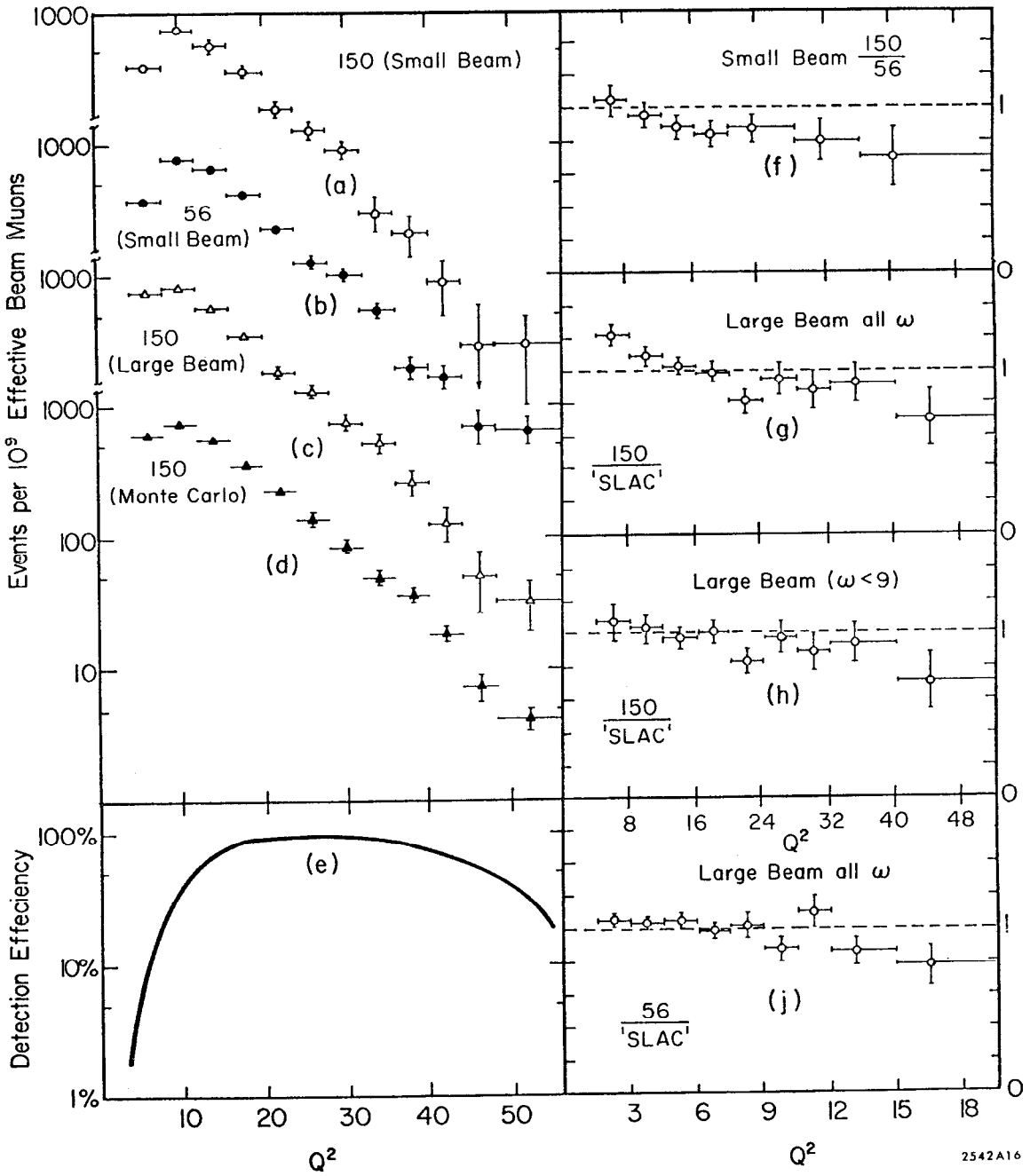
Events per 10^9 Effective Beam Muons
1000
1000
1000
1000
100
10
150 (Small Beam)
(a)
56
(Small Beam)
(b)
150
(Large Beam)
(c)
150
(Monte Carlo)
(d)
Small Beam $\frac{150}{56}$
(f)
Large Beam all ω
(g)
$\frac{150}{'SLAC'}$
Large Beam (ω<9)
(h)
$\frac{150}{'SLAC'}$
Large Beam all ω
(j)
$\frac{56}{'SLAC'}$
Detection Effeciency
100%
10%
1%
(e)
10
20
30
40
50
Q^2
8
16
24
32
40
48
Q^2
3
6
9
12
15
18
Q^2
2542A16

Fig. 7

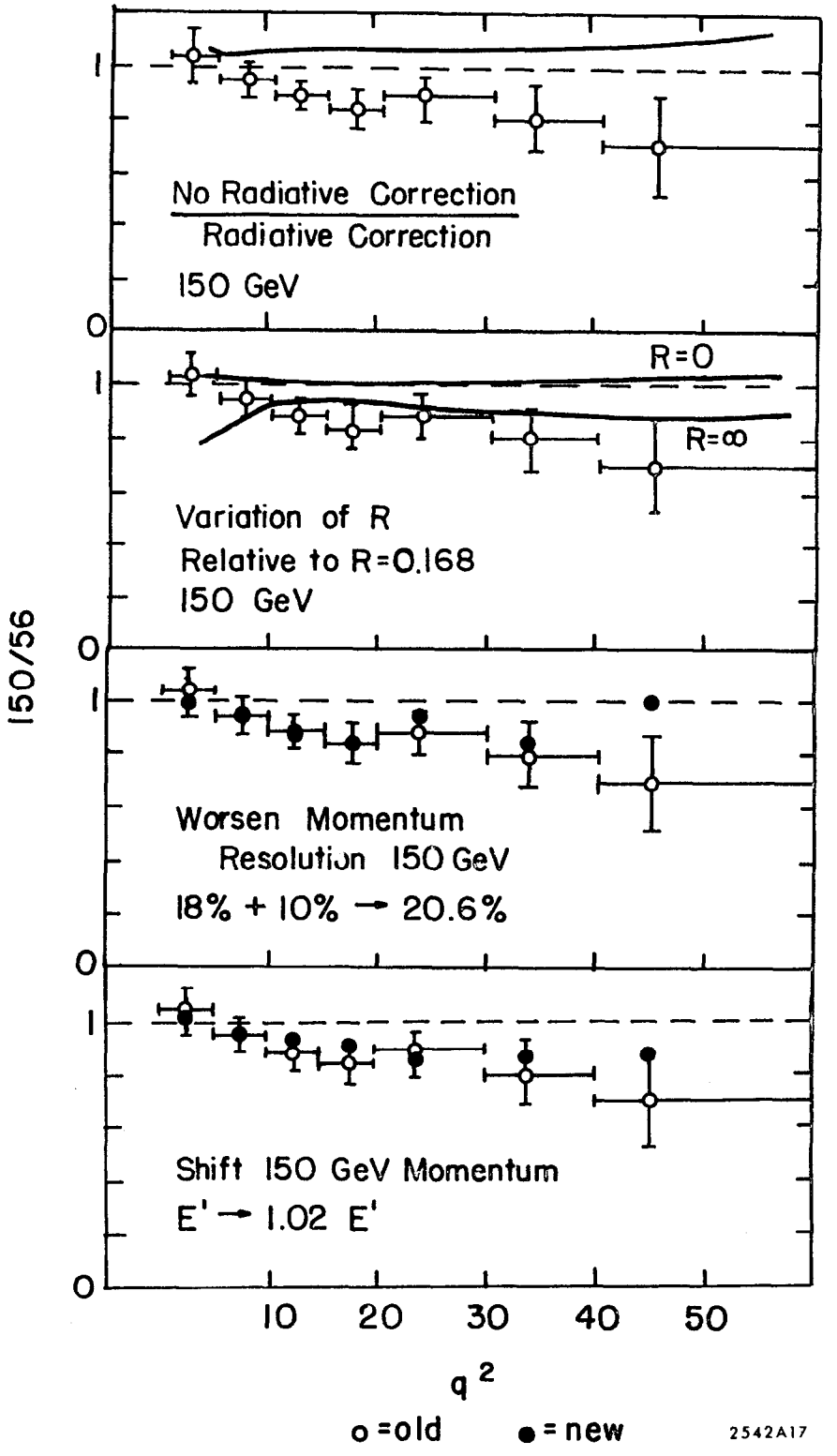
No Radiative Correction
Radiative Correction
150 GeV
R=0
R=∞
Variation of R
Relative to R=0.168
150 GeV
Worsen Momentum
Resolution 150 GeV
18% + 10% → 20.6%
Shift 150 GeV Momentum
E' → 1.02 E'
150/56
1
0
10
20
30
40
50
q 2
o =old
● = new
2542A17

Fig. 8

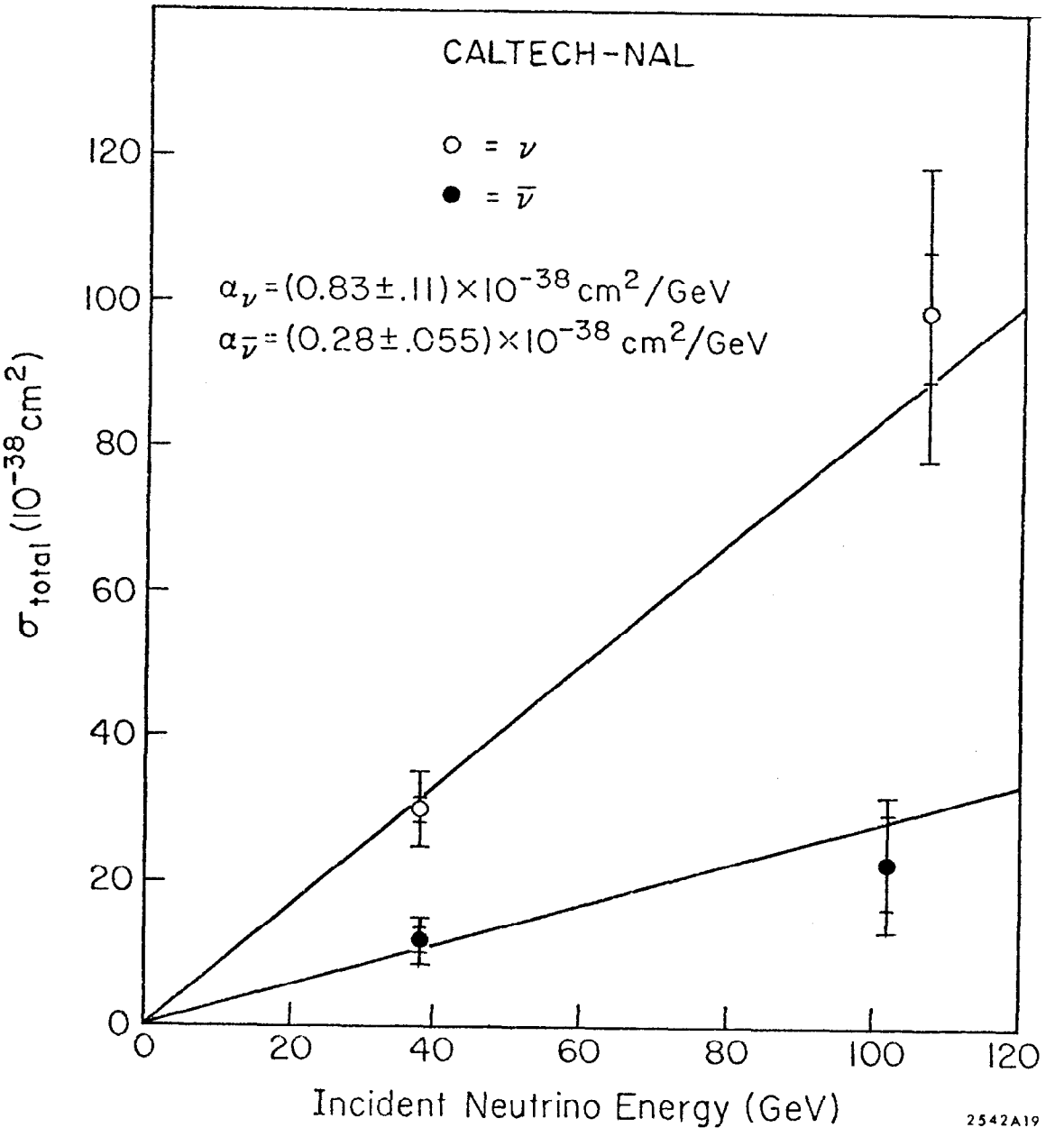
CALTECH-NAL
○ = ν
● = ν̄
αν = (0.83±.11)×10⁻³⁸ cm²/GeV
αν̄ = (0.28±.055)×10⁻³⁸ cm²/GeV
σtotal (10⁻³⁸ cm²)
0
20
40
60
80
100
120
Incident Neutrino Energy (GeV)
2542A19

Fig. 9

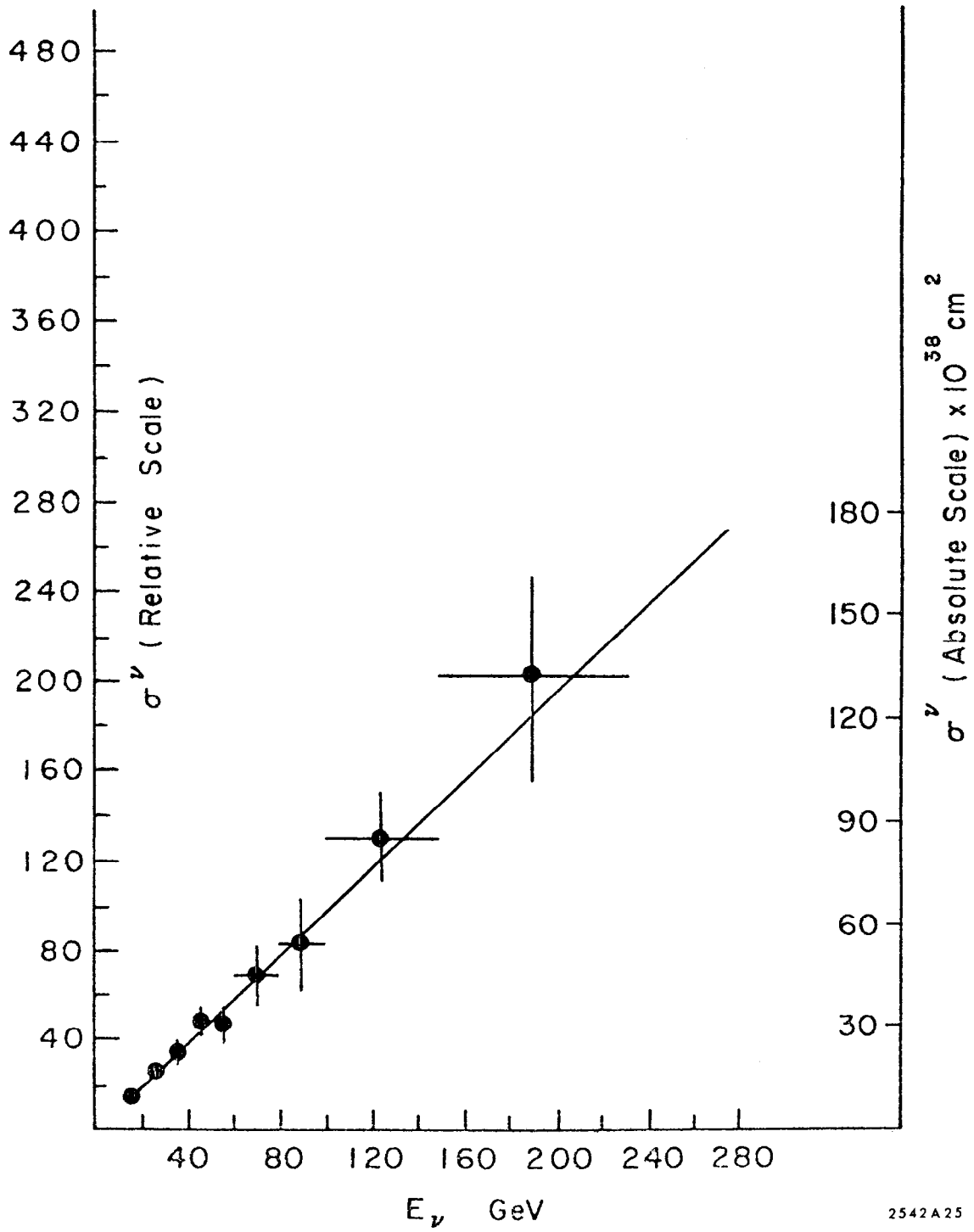
480
440
400
360
320
280
240
200
160
120
80
40
σ^ν (Relative Scale)
180
150
120
90
60
30
σ^ν (Absolute Scale) x 10^38 cm^2
40
80
120
160
200
240
280
E_ν GeV
2542A25

Fig. 10

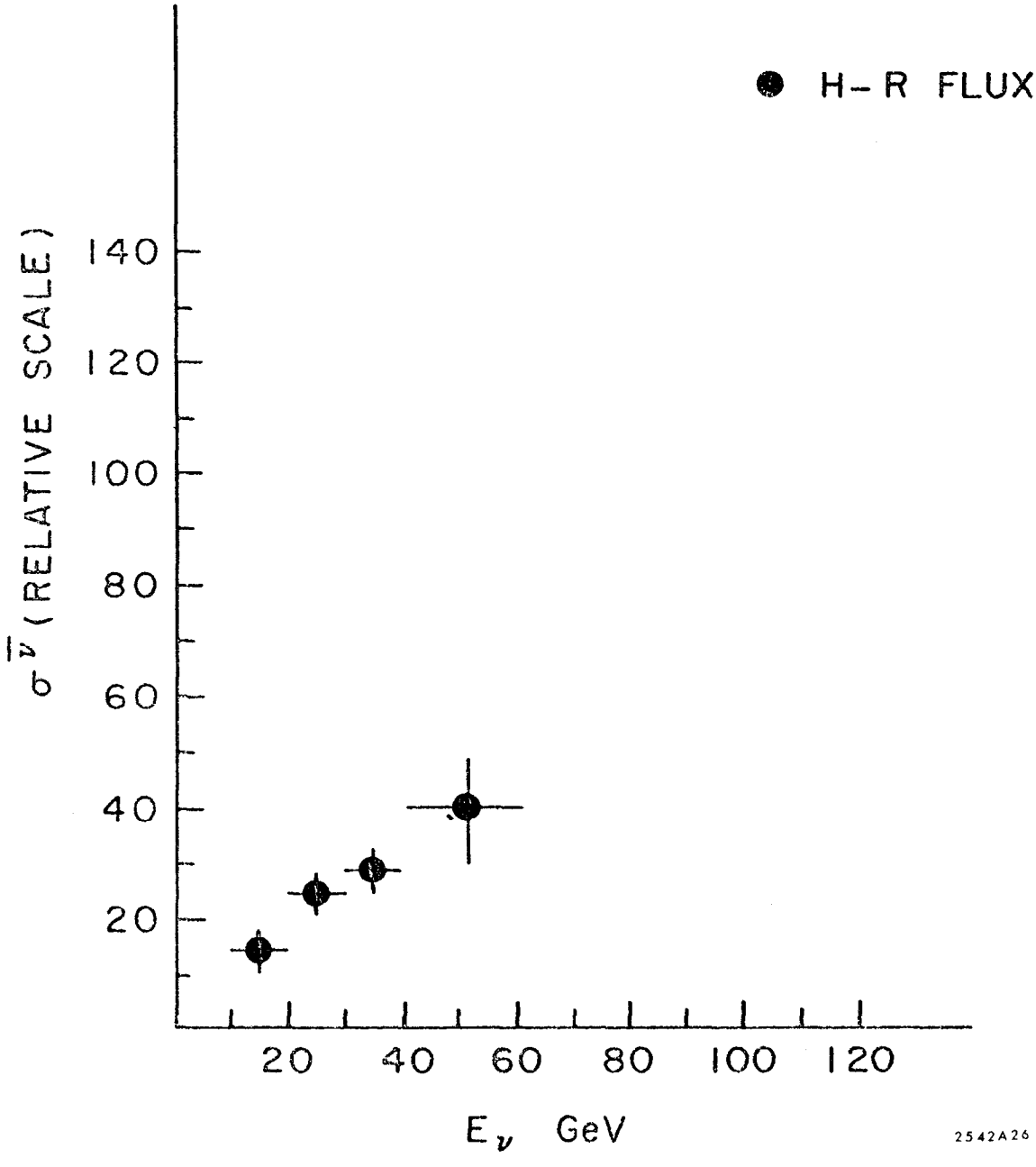
H-R FLUX
$\sigma^{\bar{\nu}}$ (RELATIVE SCALE)
140
120
100
80
60
40
20
20
40
60
80
100
120
E_ν GeV
2542A26

Fig. 11

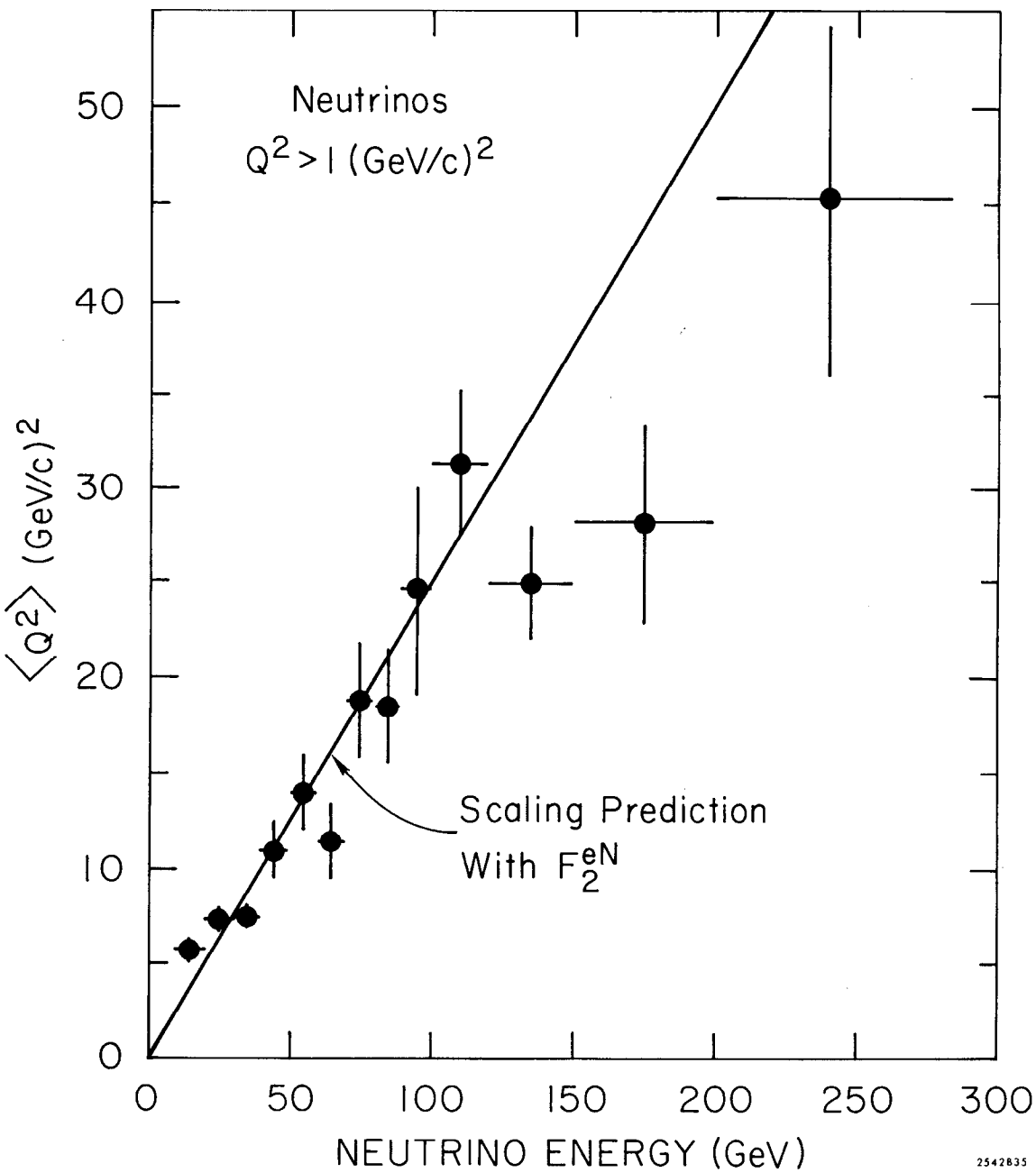
Neutrinos
$Q^2 > 1\ (GeV/c)^2$
Scaling Prediction
With F_2^{eN}
$\langle Q^2 \rangle\ (GeV/c)^2$
NEUTRINO ENERGY (GeV)
0
10
20
30
40
50
0
50
100
150
200
250
300
2542B35

Fig. 12

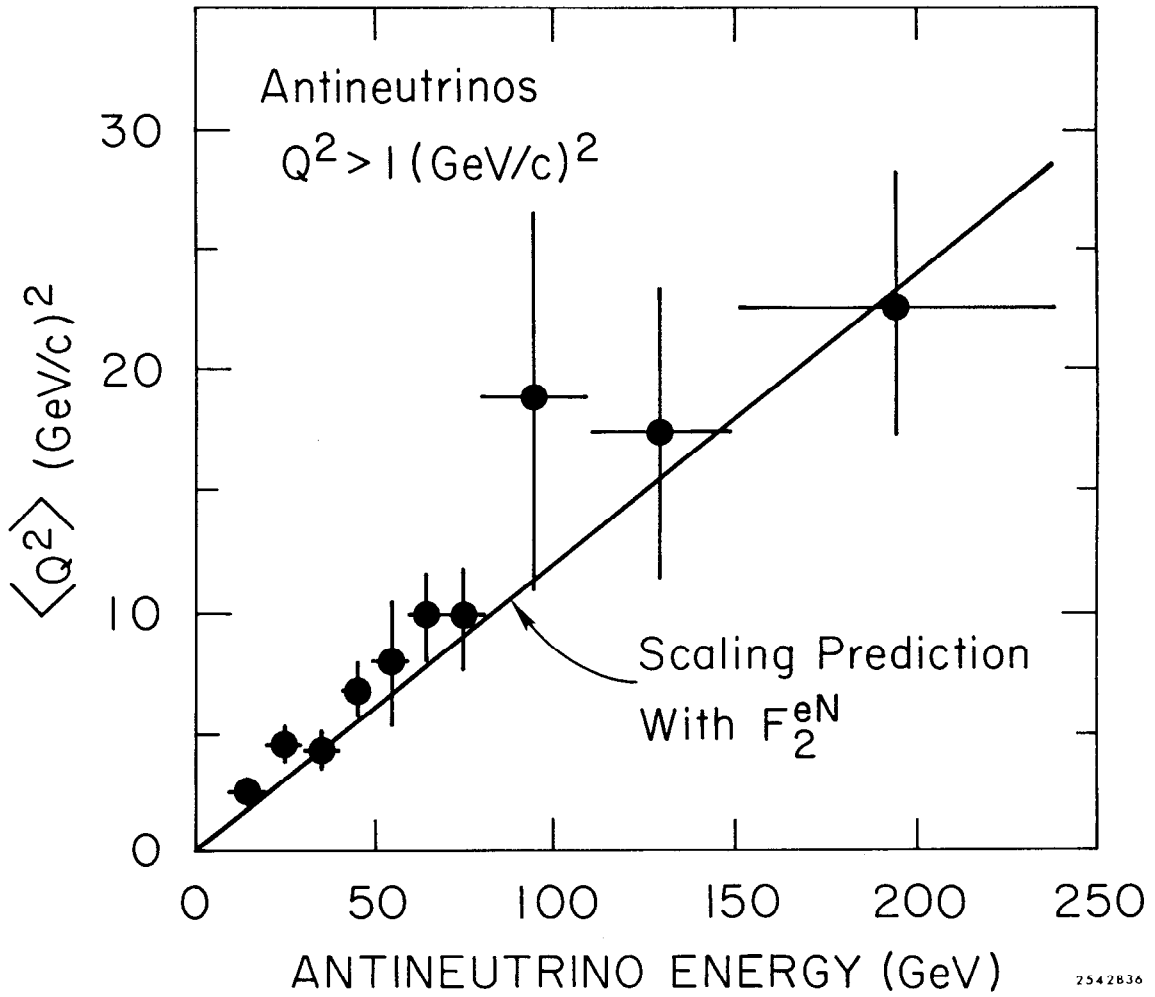
Antineutrinos
$Q^2 > 1\,(\mathrm{GeV}/c)^2$
Scaling Prediction
With F_2^{eN}
$\langle Q^2 \rangle$ $(\mathrm{GeV}/c)^2$
0
10
20
30
0
50
100
150
200
250
ANTINEUTRINO ENERGY (GeV)
2542B36

Fig. 13

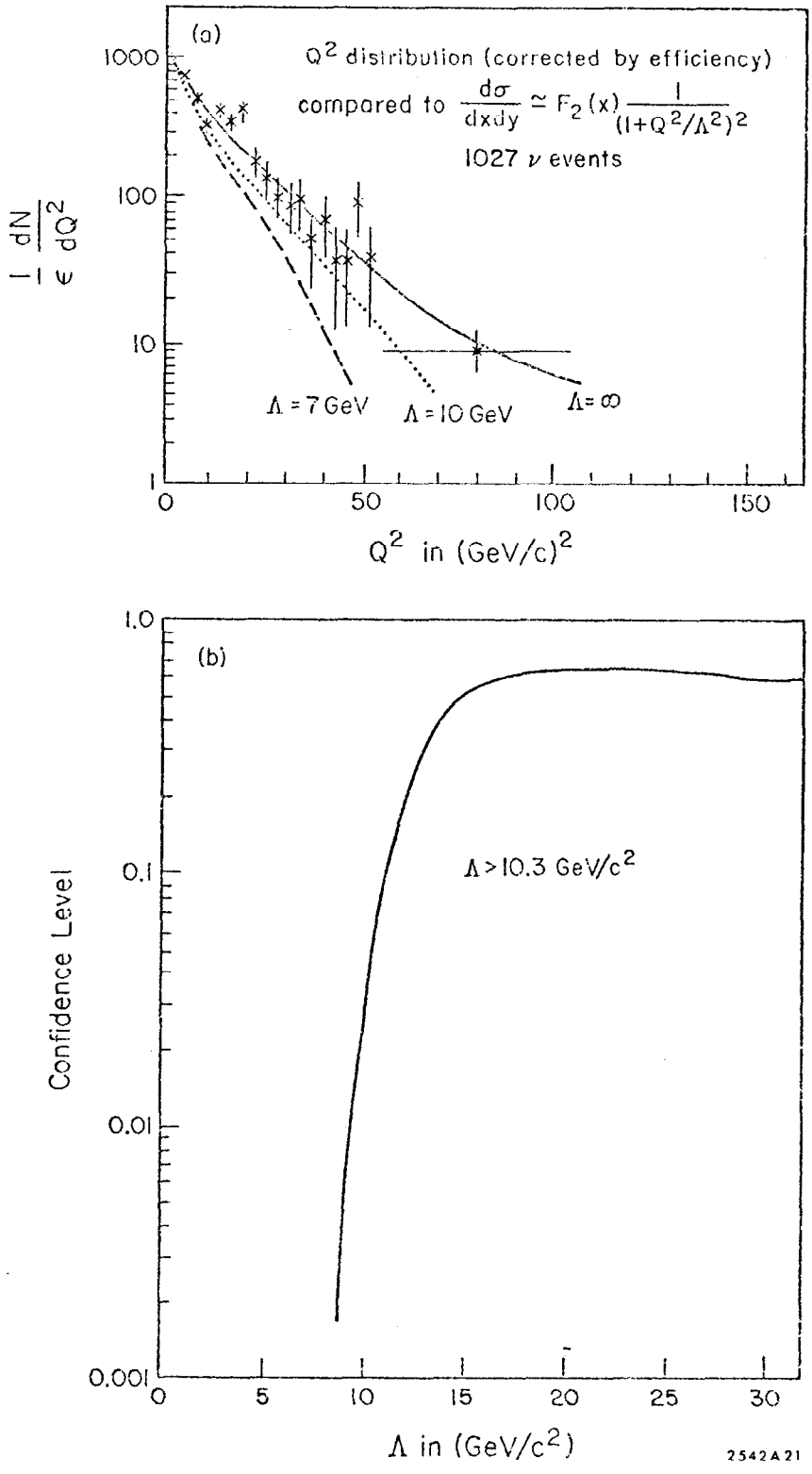
(a)
Q^2 distribution (corrected by efficiency)
compared to $\frac{d\sigma}{dxdy} \simeq F_2(x) \frac{1}{(1+Q^2/\Lambda^2)^2}$
1027 ν events
$\frac{1}{\epsilon}\frac{dN}{dQ^2}$
1000
100
10
1
0
50
100
150
Λ = 7 GeV
Λ = 10 GeV
$\Lambda = \infty$
Q^2 in $(GeV/c)^2$
(b)
Confidence Level
1.0
0.1
0.01
0.001
0
5
10
15
20
25
30
$\Lambda > 10.3$ GeV/c^2
Λ in (GeV/c^2)
2542A21

Fig. 14

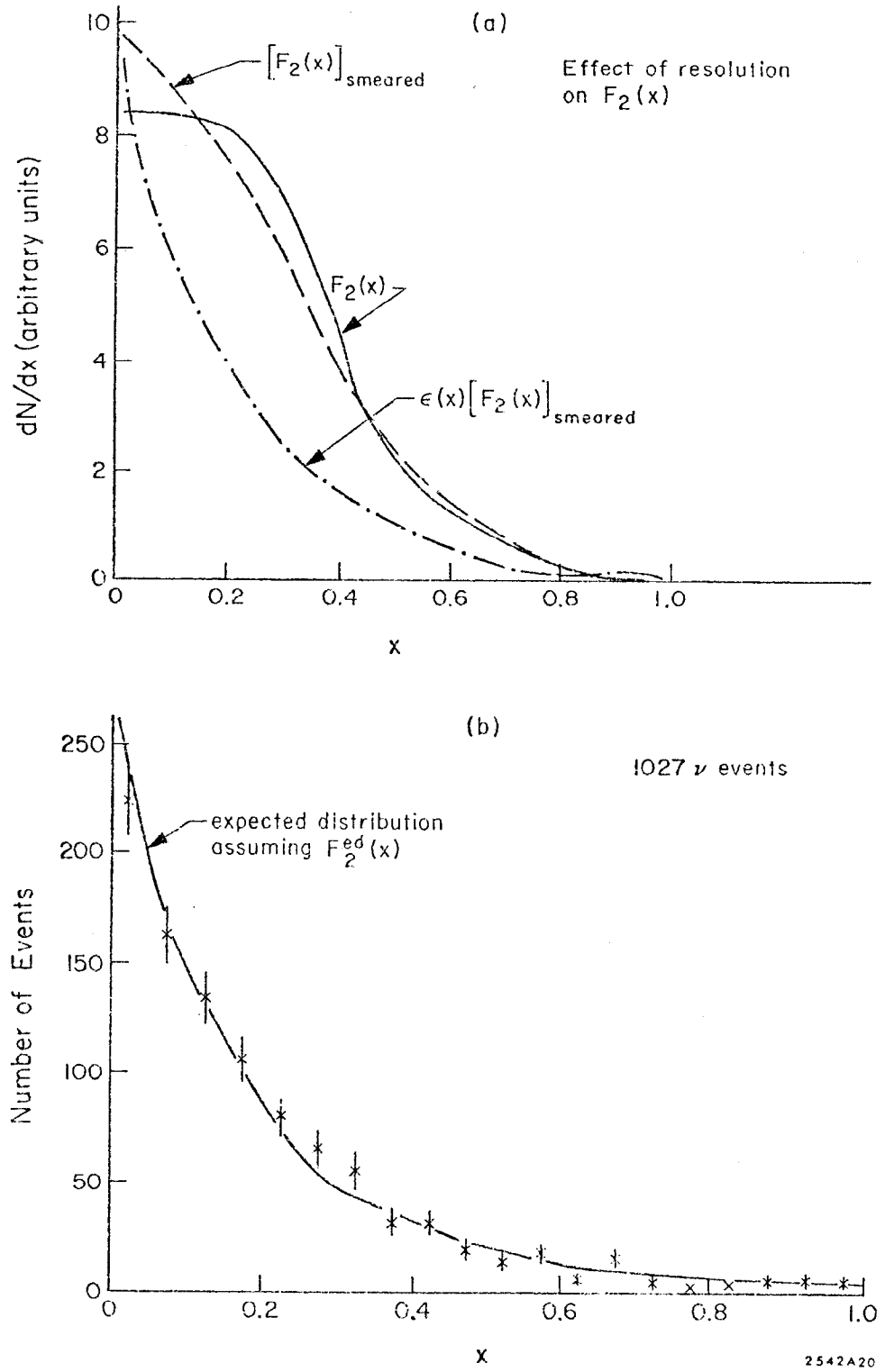
(a)
Effect of resolution on $F_2(x)$
$[F_2(x)]_{smeared}$
$F_2(x)$
$\epsilon(x)[F_2(x)]_{smeared}$
dN/dx (arbitrary units)
x
(b)
1027 ν events
expected distribution assuming $F_2^{ed}(x)$
Number of Events
x
2542A20

Fig. 15

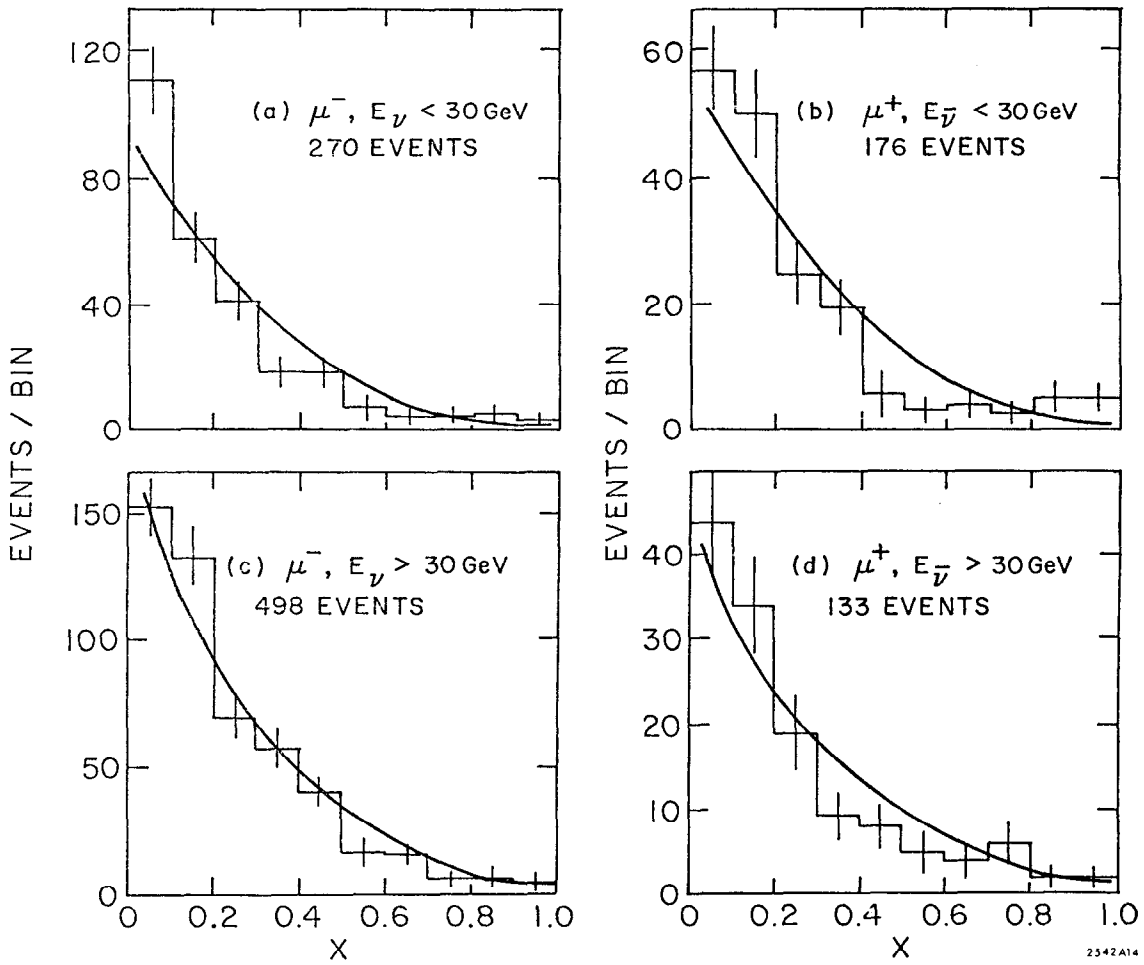
(a) μ^-, E_ν < 30 GeV
270 EVENTS
(b) μ^+, $E_{\bar{\nu}}$ < 30 GeV
176 EVENTS
(c) μ^-, E_ν > 30 GeV
498 EVENTS
(d) μ^+, $E_{\bar{\nu}}$ > 30 GeV
133 EVENTS
EVENTS / BIN
X
2342A14

Fig. 16

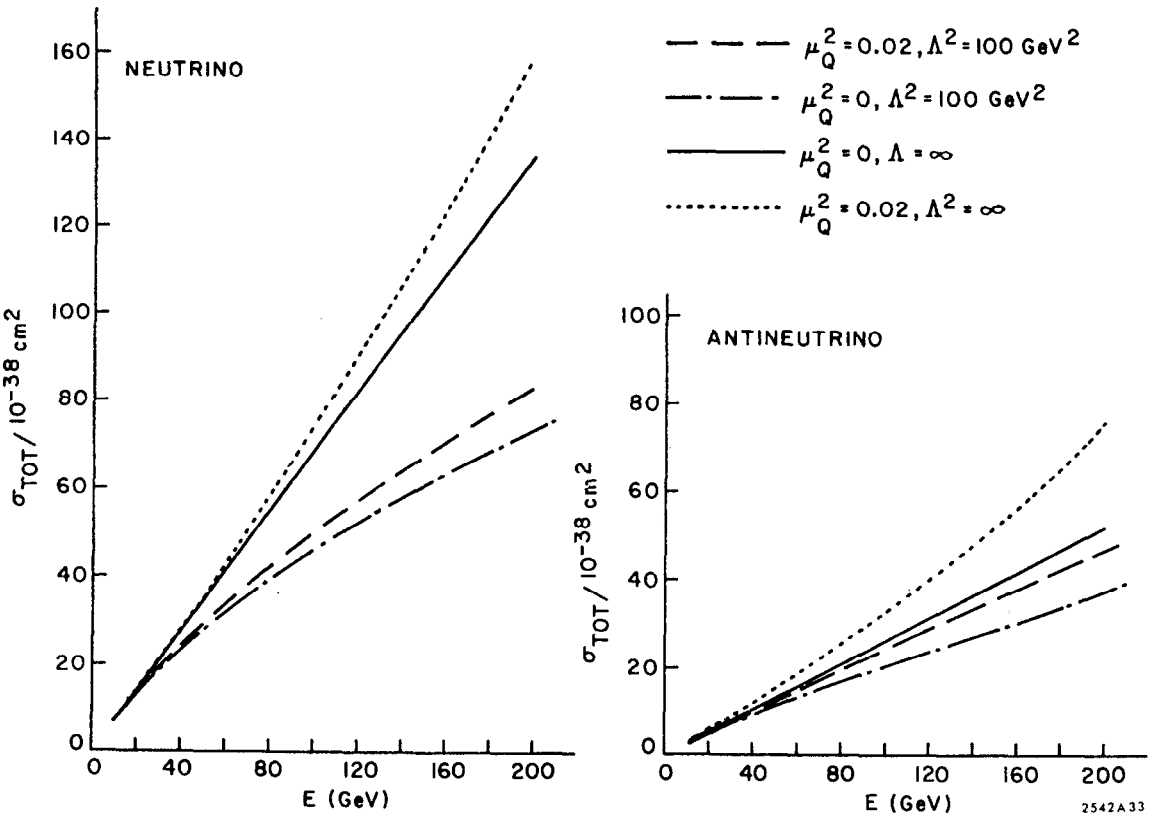
NEUTRINO
ANTINEUTRINO
$\mu_Q^2 = 0.02, \Lambda^2 = 100\ \mathrm{GeV}^2$
$\mu_Q^2 = 0, \Lambda^2 = 100\ \mathrm{GeV}^2$
$\mu_Q^2 = 0, \Lambda = \infty$
$\mu_Q^2 = 0.02, \Lambda^2 = \infty$
$\sigma_{TOT} / 10^{-38}\ \mathrm{cm}^2$
E (GeV)
2542A33

Fig. 17

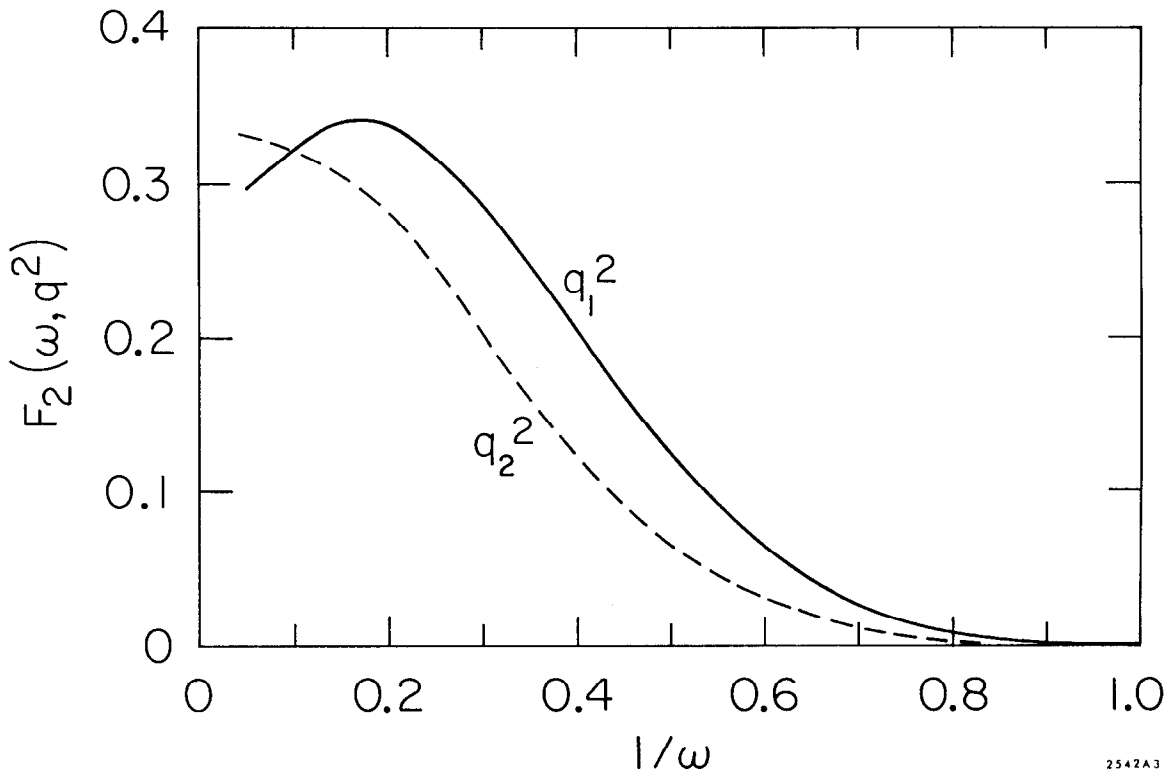

Fig. 18

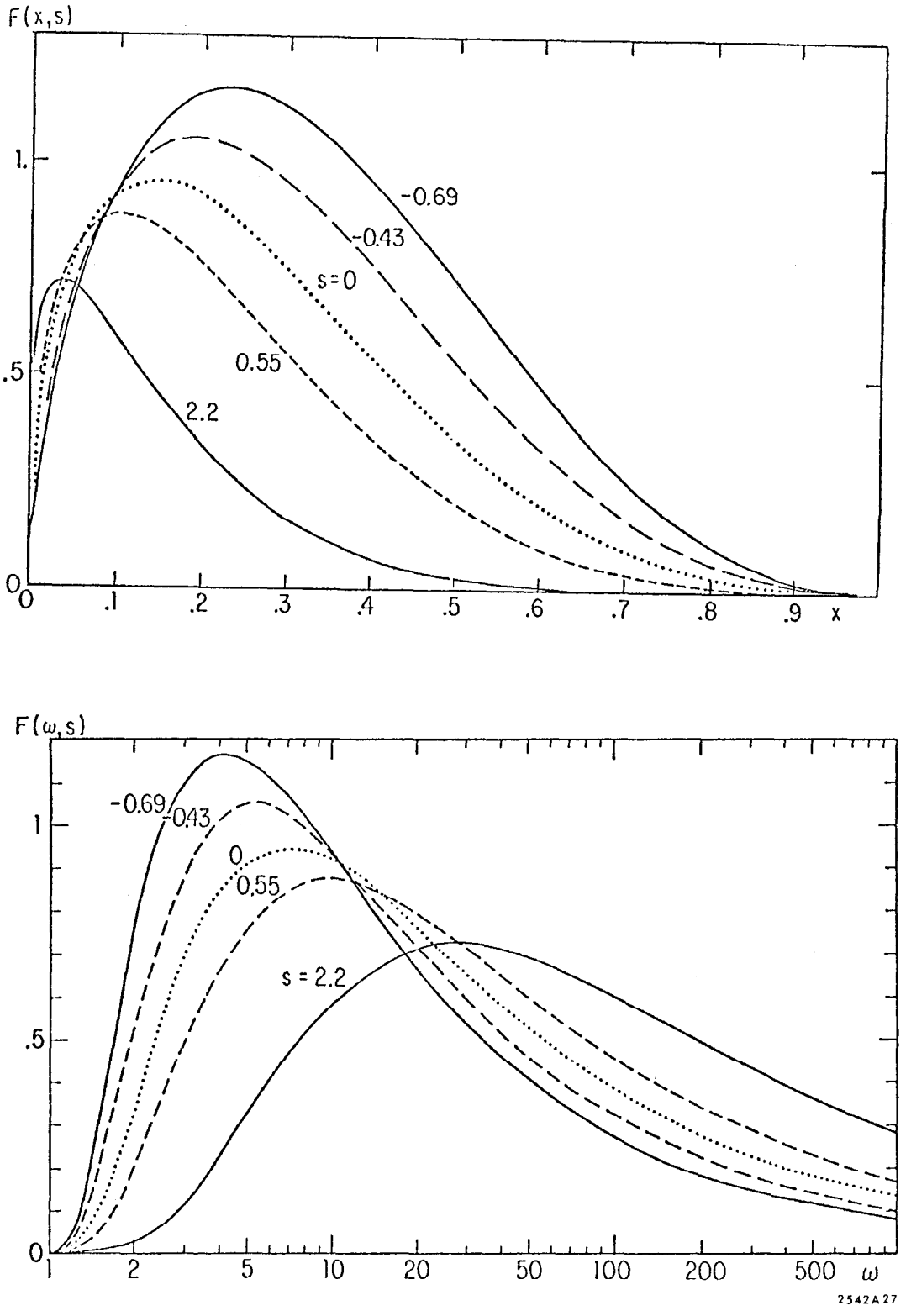
F(x,s)
1.
.5
0
0
.1
.2
.3
.4
.5
.6
.7
.8
.9
x
-0.69
-0.43
s=0
0.55
2.2
F(ω,s)
1
.5
0
1
2
5
10
20
50
100
200
500
ω
-0.69
-0.43
0
0.55
s = 2.2
2542A27

Fig. 19

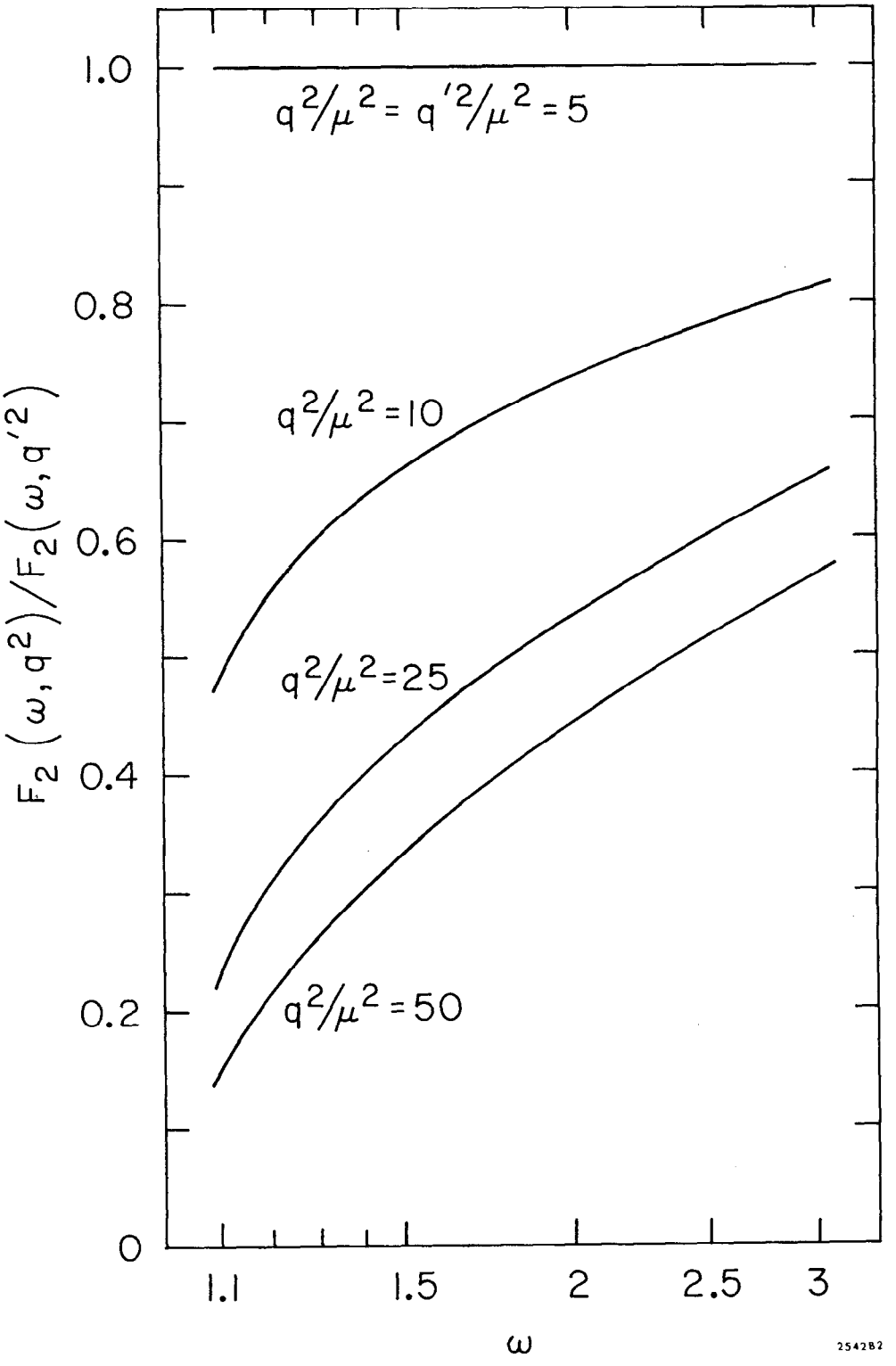
1.0
0.8
0.6
0.4
0.2
0
$q^2/\mu^2 = q'^2/\mu^2 = 5$
$q^2/\mu^2 = 10$
$q^2/\mu^2 = 25$
$q^2/\mu^2 = 50$
$F_2(\omega, q^2)/F_2(\omega, q'^2)$
1.1
1.5
2
2.5
3
ω
2542B2

Fig. 20

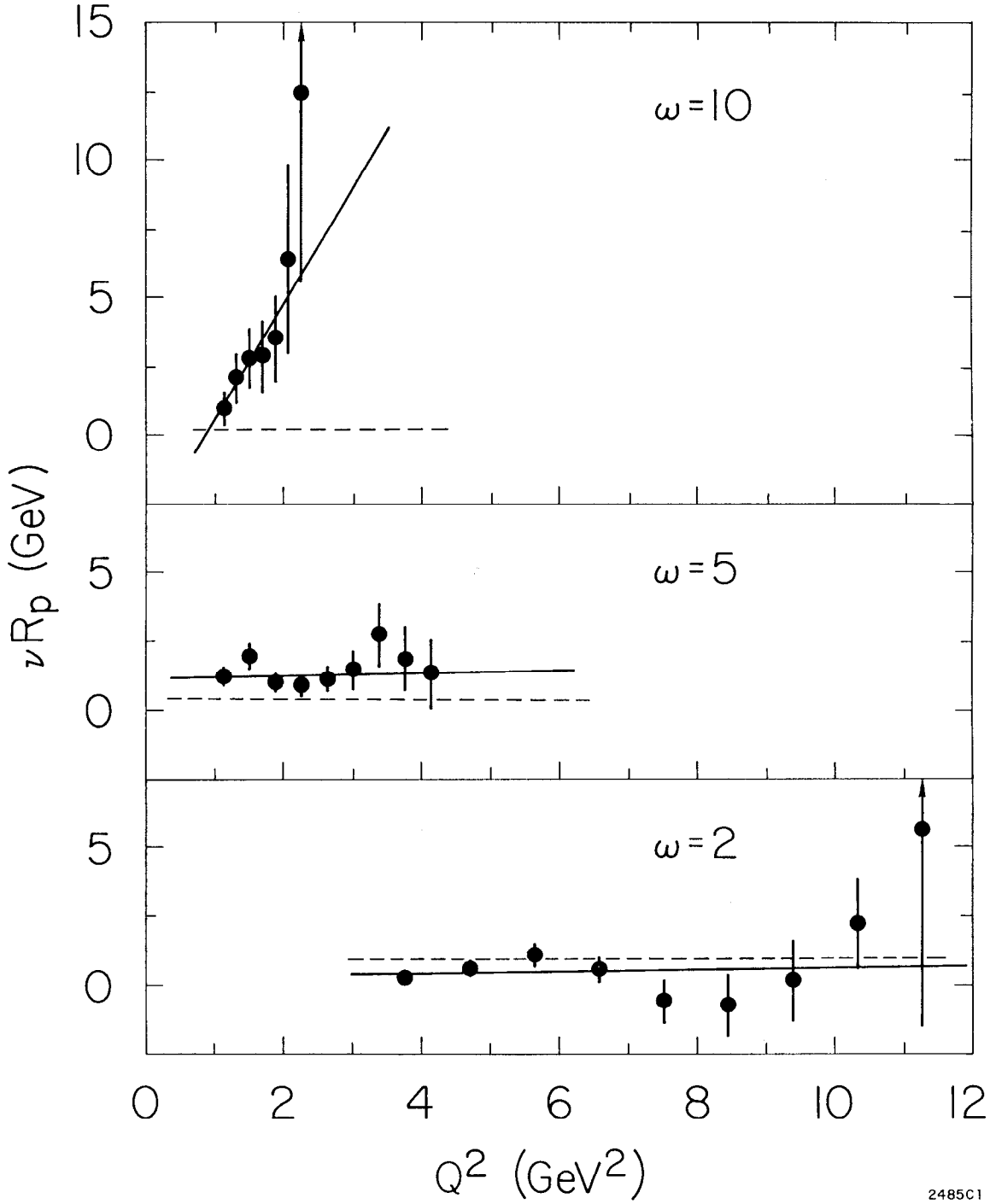

Fig. 21

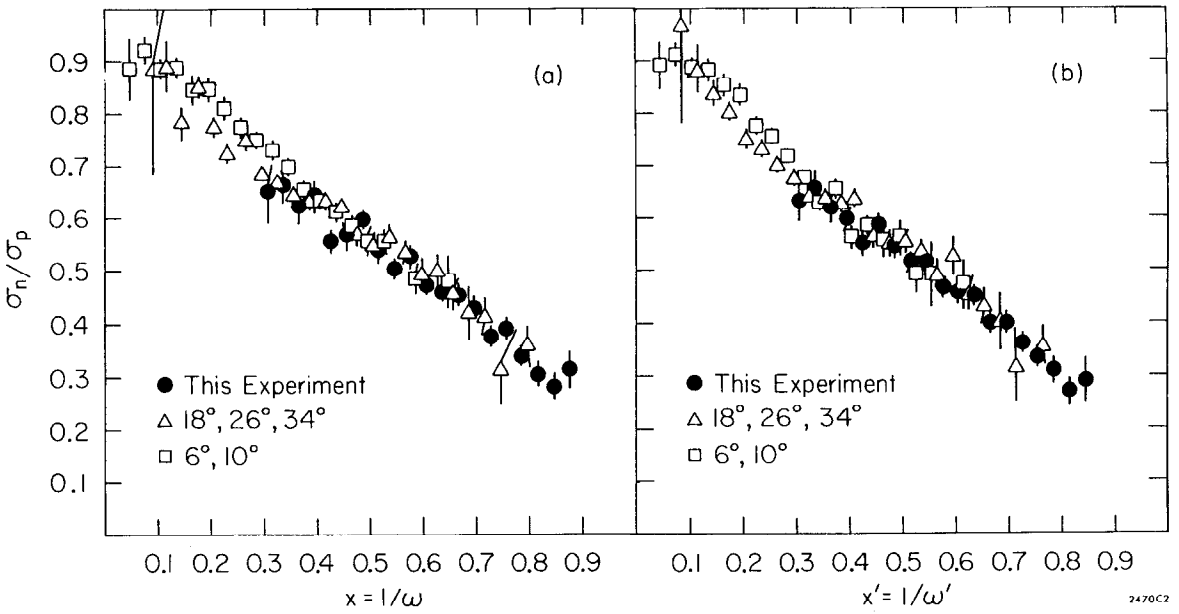
(a)
(b)
σ_n/σ_p
0.9
0.8
0.7
0.6
0.5
0.4
0.3
0.2
0.1
● This Experiment
△ 18°, 26°, 34°
□ 6°, 10°
0.1 0.2 0.3 0.4 0.5 0.6 0.7 0.8 0.9
$x = 1/\omega$
$x' = 1/\omega'$
2470C2

Fig. 22

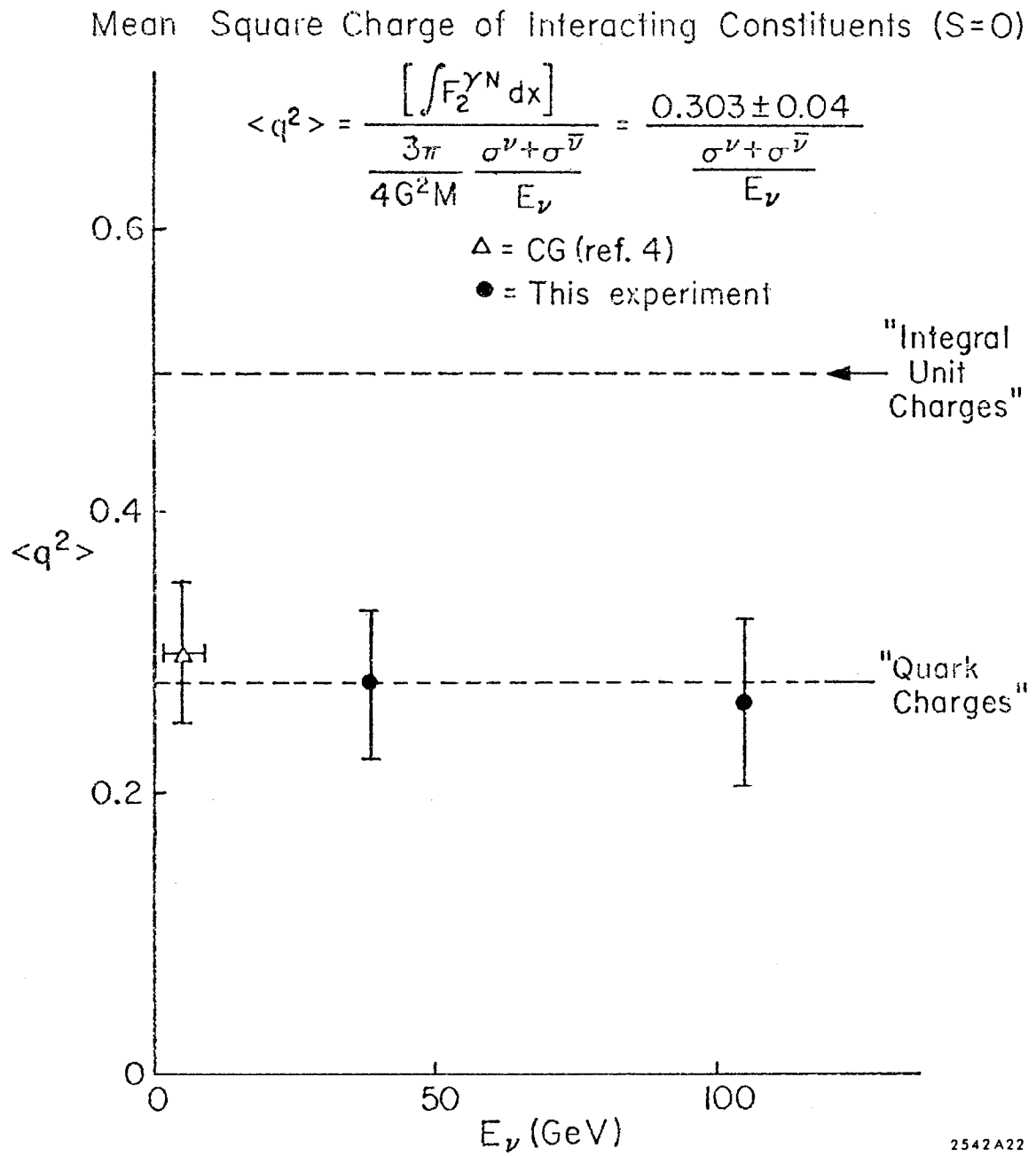
Mean Square Charge of Interacting Constituents (S=O)
$\langle q^2 \rangle = \frac{\left[\int F_2^{\gamma N} dx\right]}{\frac{3\pi}{4G^2M}\frac{\sigma^\nu+\sigma^{\bar\nu}}{E_\nu}} = \frac{0.303 \pm 0.04}{\frac{\sigma^\nu+\sigma^{\bar\nu}}{E_\nu}}$
Δ = CG (ref. 4)
● = This experiment
"Integral Unit Charges"
"Quark Charges"
$\langle q^2 \rangle$
0.6
0.4
0.2
0
0
50
100
E_ν (GeV)
2542A22

Fig. 23

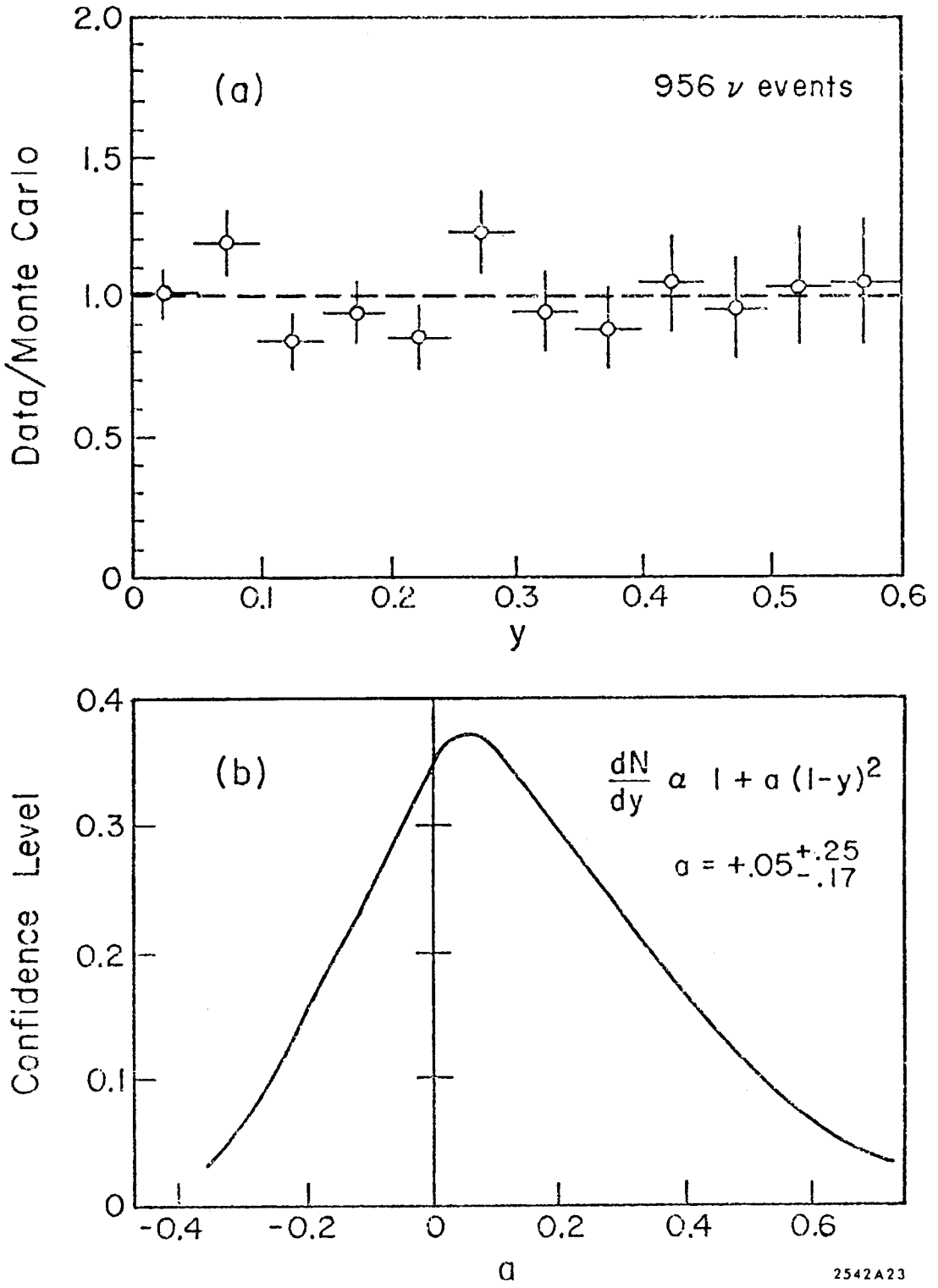
(a)
956 ν events
Data/Monte Carlo
2.0
1.5
1.0
0.5
0
0
0.1
0.2
0.3
0.4
0.5
0.6
y
(b)
$\frac{dN}{dy} \propto 1 + a(1-y)^2$
$a = +.05^{+.25}_{-.17}$
Confidence Level
0.4
0.3
0.2
0.1
0
-0.4
-0.2
0
0.2
0.4
0.6
a
2542A23

Fig. 24

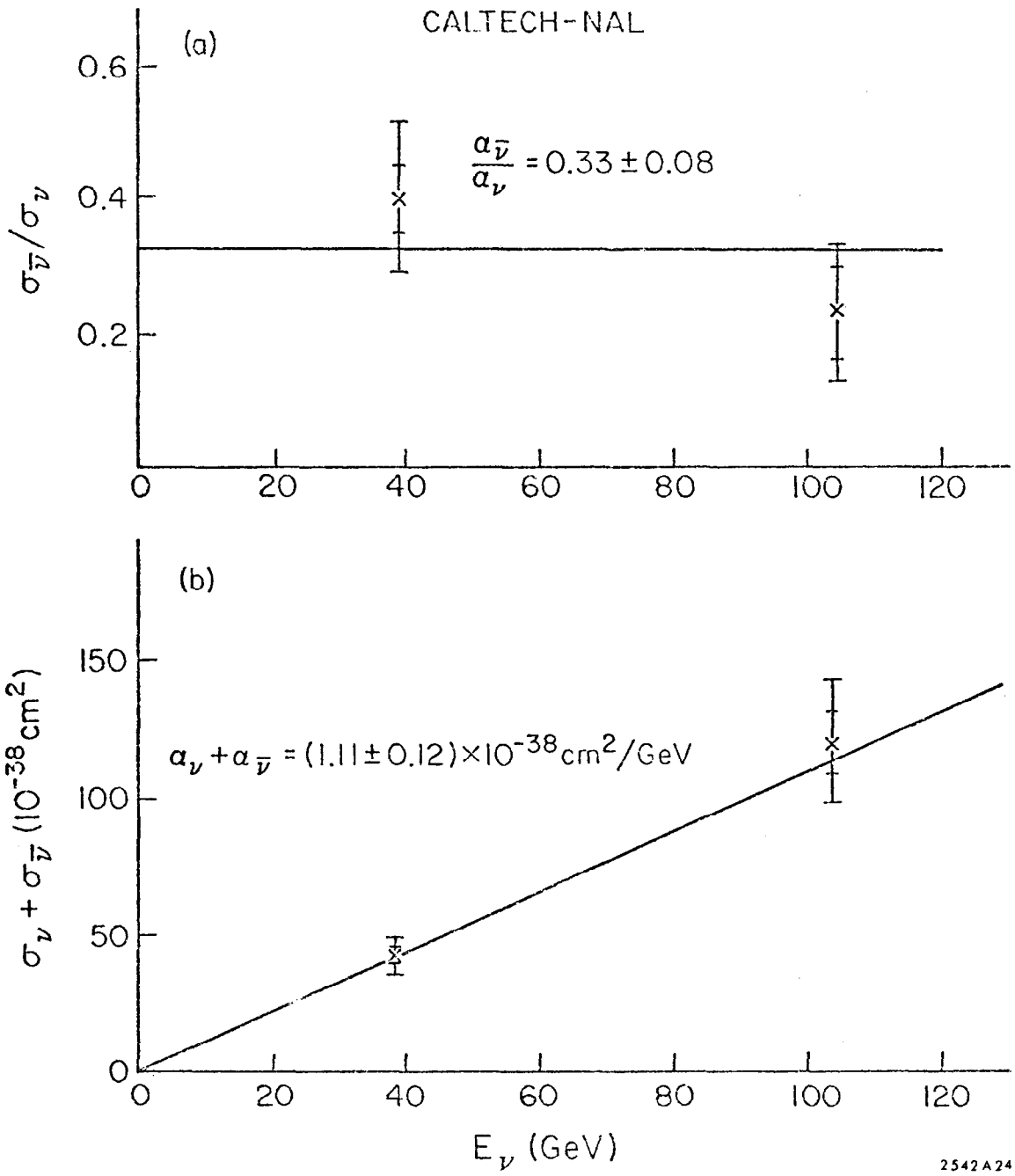
CALTECH-NAL
(a)
0.6
0.4
0.2
$\sigma_{\bar{\nu}}/\sigma_{\nu}$
$\frac{\alpha_{\bar{\nu}}}{\alpha_{\nu}} = 0.33 \pm 0.08$
0
20
40
60
80
100
120
(b)
150
100
50
0
$\sigma_{\nu} + \sigma_{\bar{\nu}}$ (10^{-38}cm^2)
$\alpha_{\nu} + \alpha_{\bar{\nu}} = (1.11 \pm 0.12) \times 10^{-38}$cm^2/GeV
0
20
40
60
80
100
120
E_{ν} (GeV)
2542A24

Fig. 25

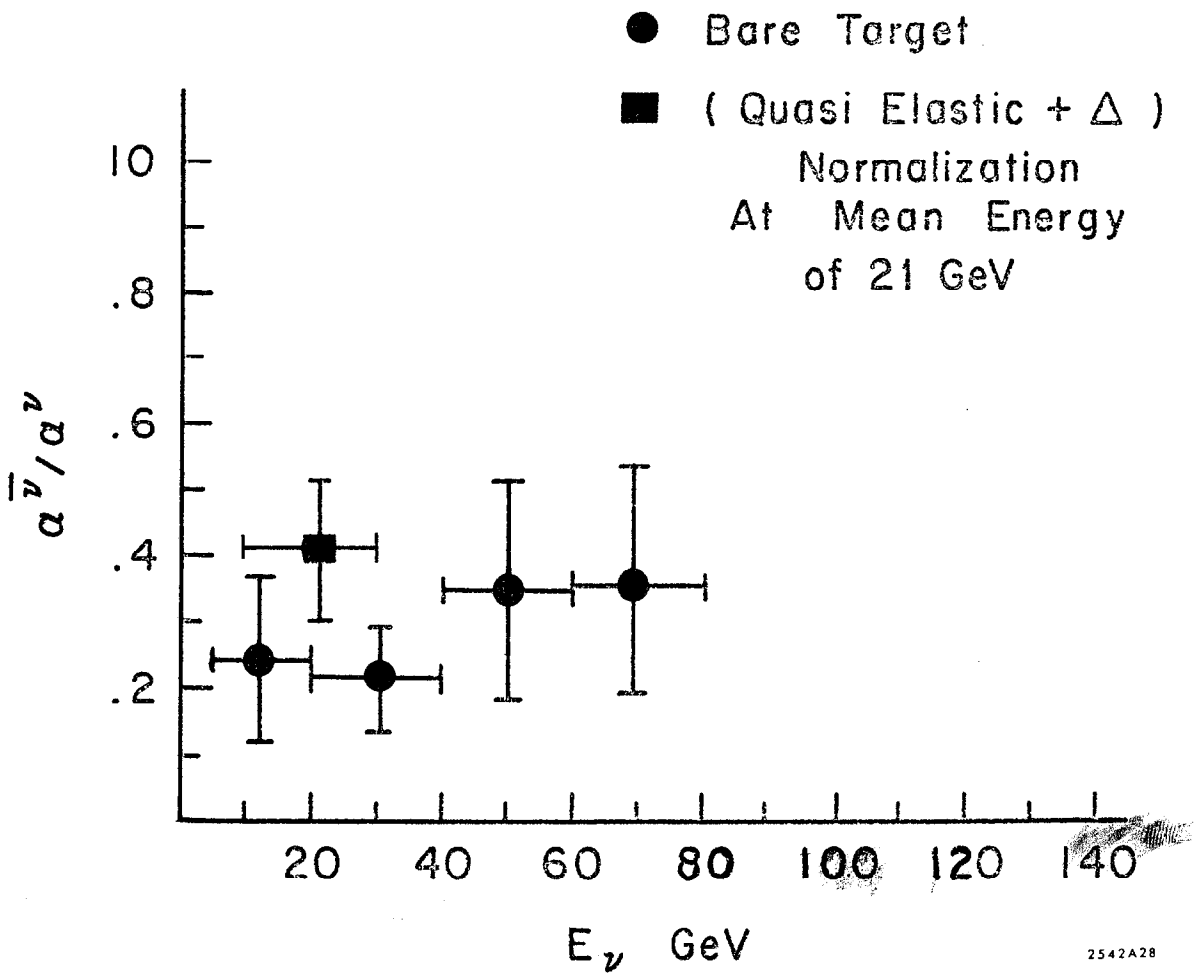
Bare Target
(Quasi Elastic + Δ)
Normalization
At Mean Energy
of 21 GeV
10
.8
.6
.4
.2
$\sigma^{\bar{\nu}}/\sigma^{\nu}$
20
40
60
80
100
120
140
E_{ν} GeV
2542A28

Fig. 26

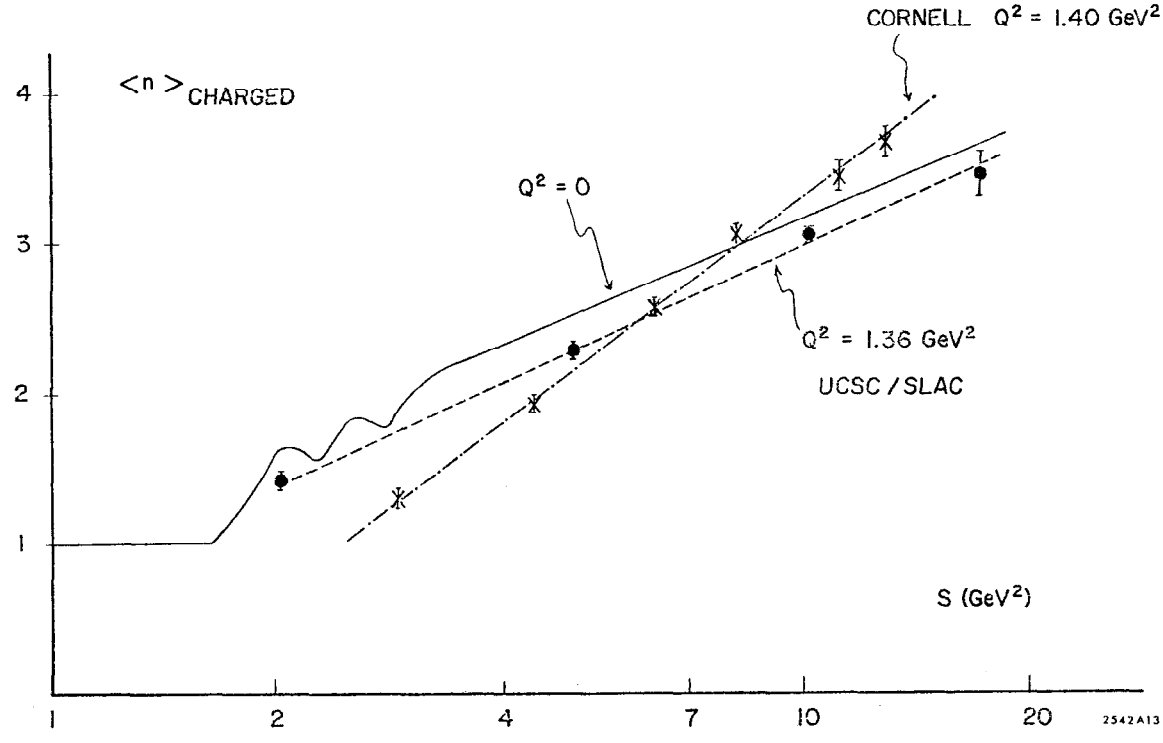
CORNELL Q² = 1.40 GeV²
<n> CHARGED
Q² = 0
Q² = 1.36 GeV²
UCSC / SLAC
S (GeV²)
4
3
2
1
1
2
4
7
10
20
2542A13

Fig. 27

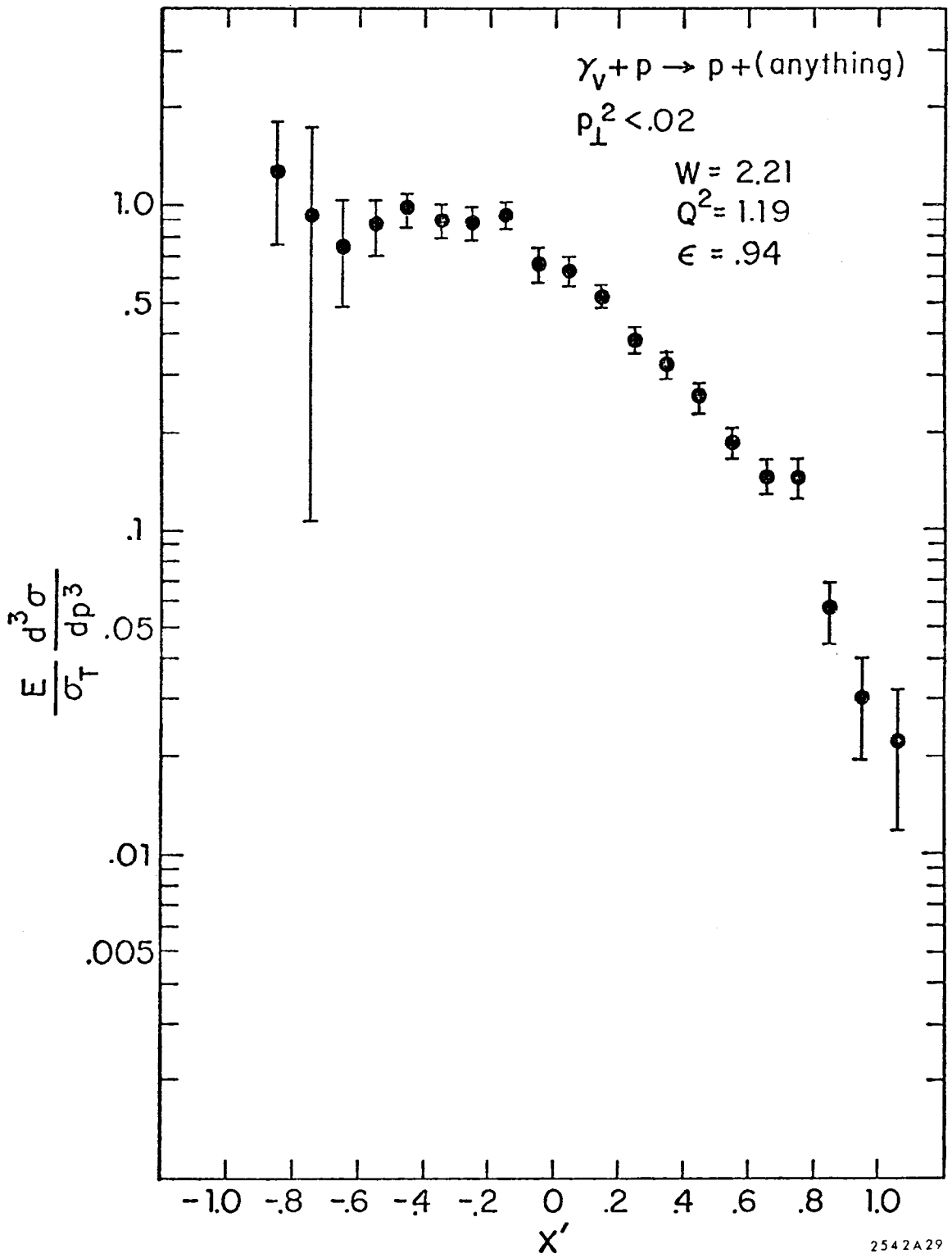
$\gamma_V + p \rightarrow p + (\text{anything})$
$p_\perp^2 < .02$
W = 2.21
Q^2 = 1.19
ϵ = .94
1.0
.5
.1
.05
.01
.005
$E \frac{d^3\sigma}{dp^3} \Big/ \sigma_T$
-1.0
-.8
-.6
-.4
-.2
0
.2
.4
.6
.8
1.0
X′
2542A29

Fig. 28

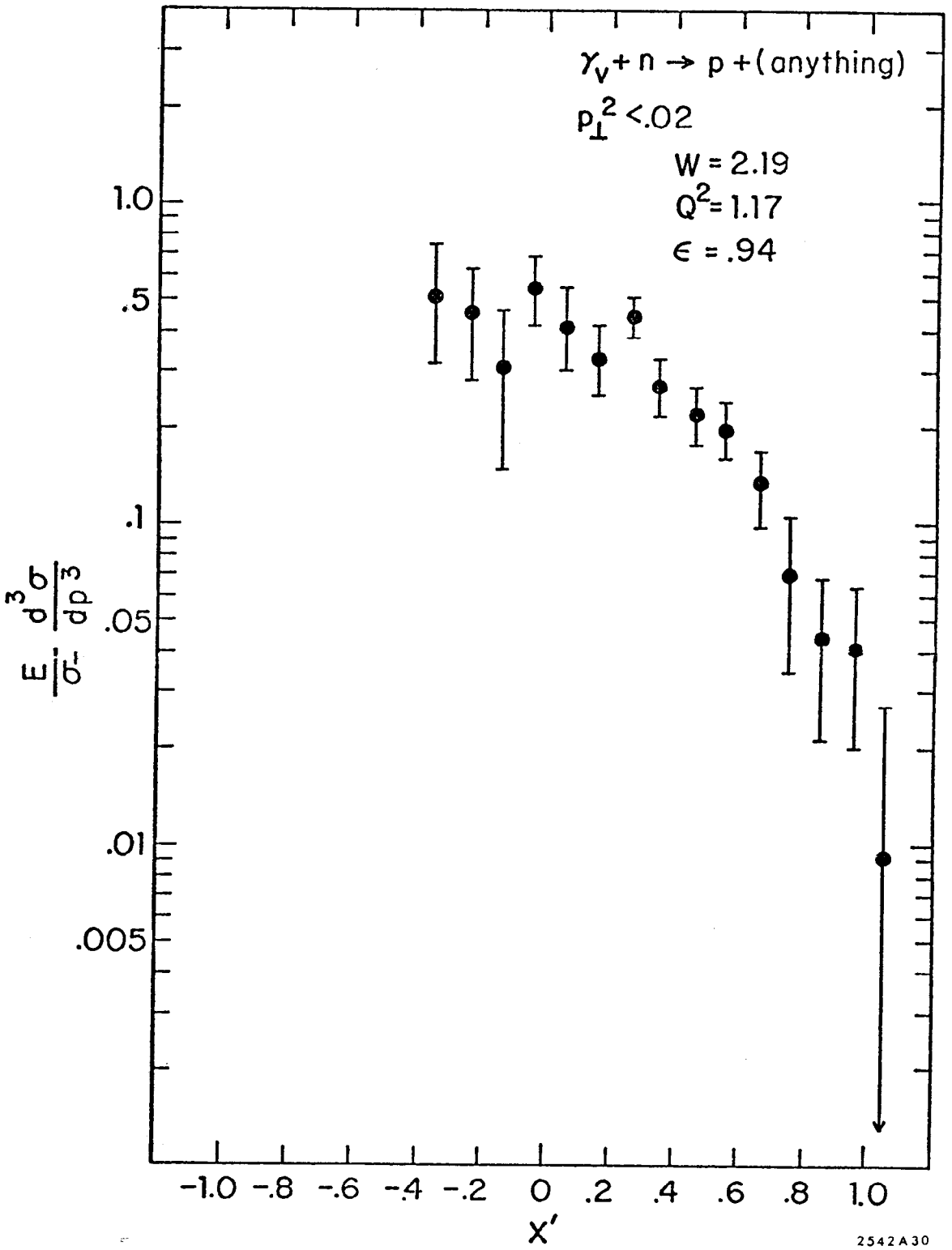
$\gamma_V + n \rightarrow p + (\text{anything})$
$p_\perp^2 < .02$
W = 2.19
$Q^2 = 1.17$
$\epsilon = .94$
1.0
.5
.1
.05
.01
.005
$E \frac{d^3\sigma}{dp^3} \Big/ \sigma_T$
-1.0 -.8 -.6 -.4 -.2 0 .2 .4 .6 .8 1.0
X'
2542A30

Fig. 29

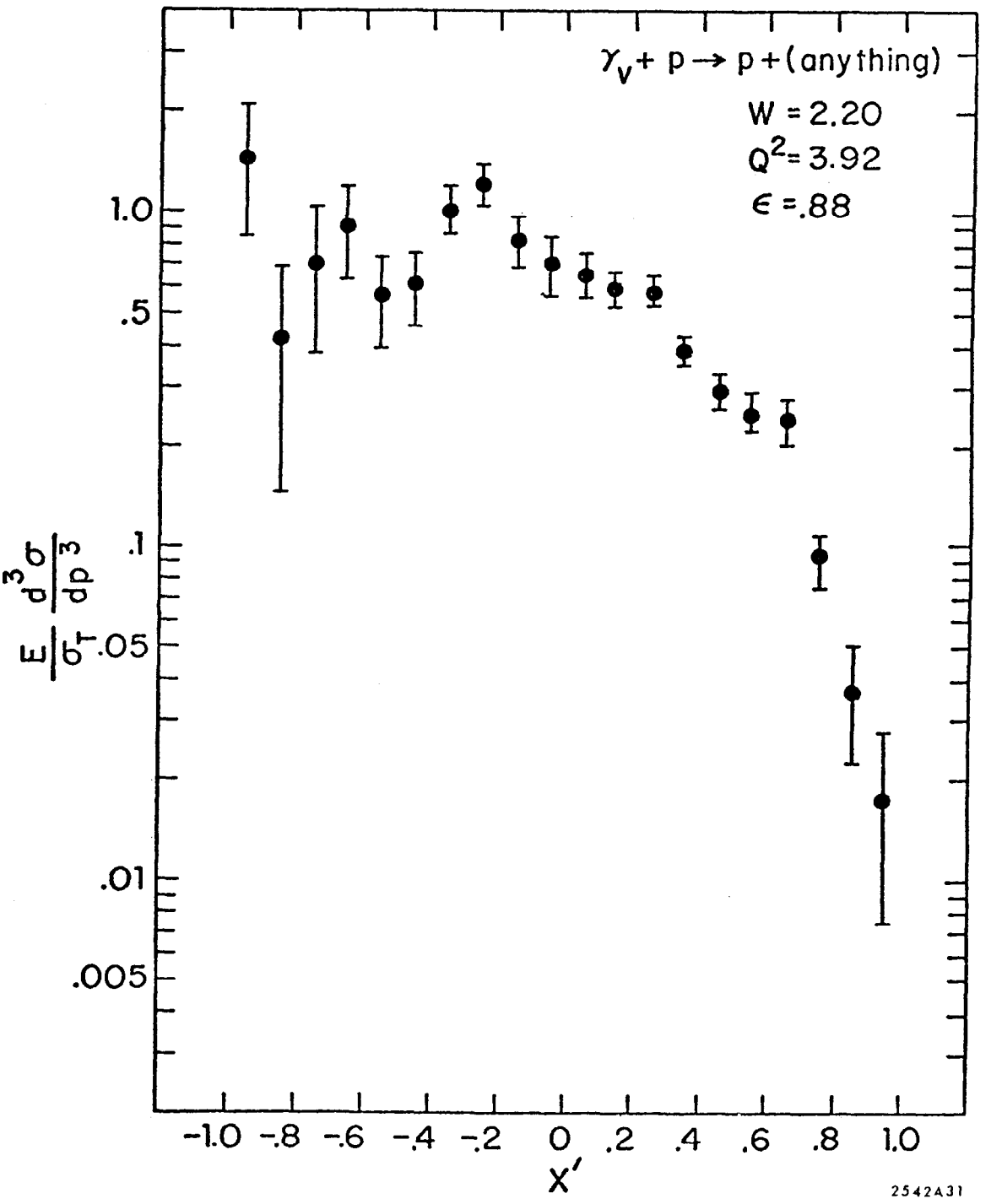
$\gamma_V + p \rightarrow p + (\text{anything})$
W = 2.20
$Q^2 = 3.92$
$\epsilon = .88$
1.0
.5
.1
.05
.01
.005
$E \frac{d^3\sigma}{dp^3} \Big/ \sigma_T$
-1.0 -.8 -.6 -.4 -.2 0 .2 .4 .6 .8 1.0
X′
2542A31

Fig. 30

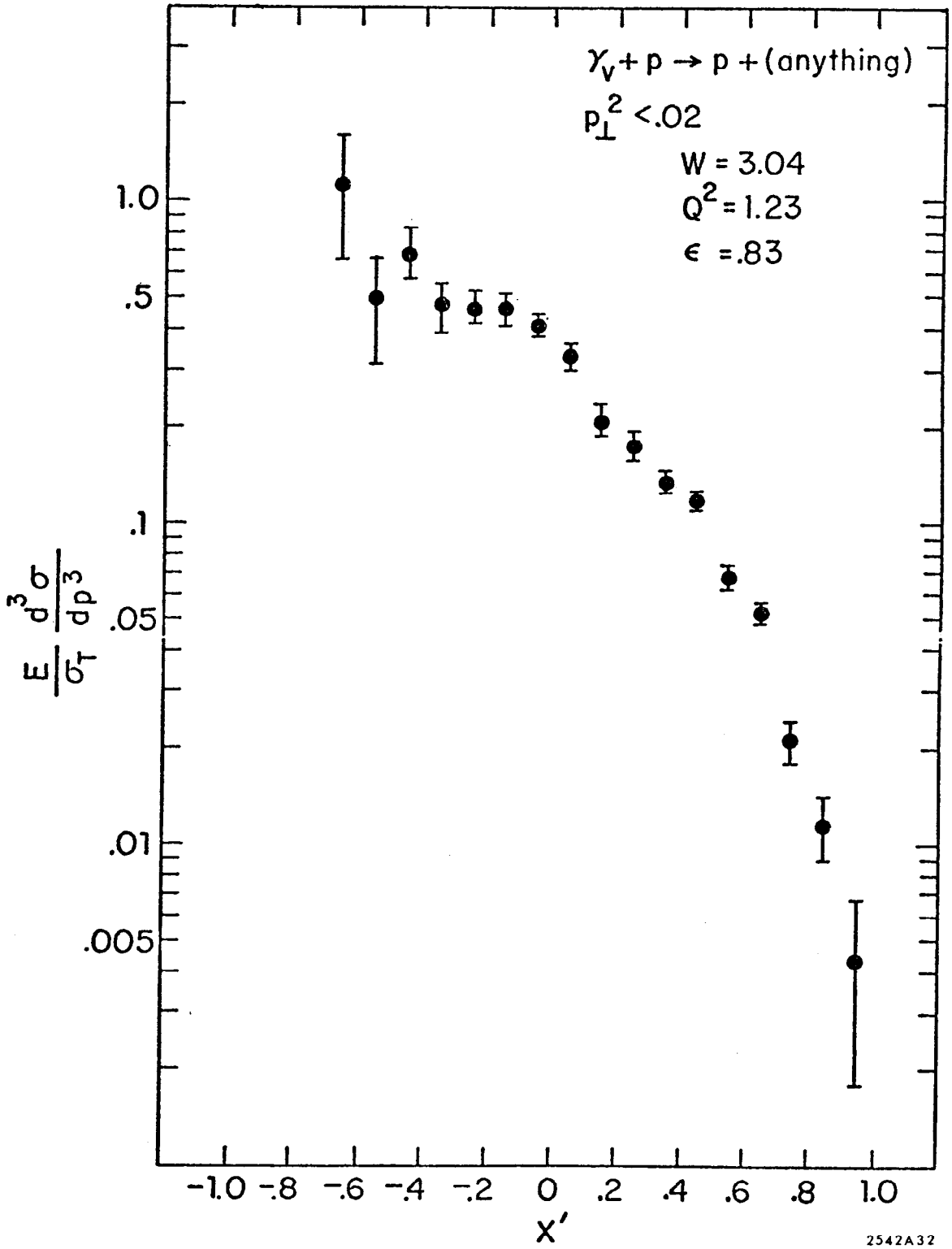
$\gamma_v + p \rightarrow p + (\text{anything})$
$p_\perp^2 < .02$
W = 3.04
$Q^2 = 1.23$
$\epsilon = .83$
1.0
.5
.1
.05
.01
.005
$E \frac{d^3\sigma}{dp^3} \Big/ \sigma_T$
-1.0 -.8 -.6 -.4 -.2 0 .2 .4 .6 .8 1.0
X'
2542A32

Fig. 31

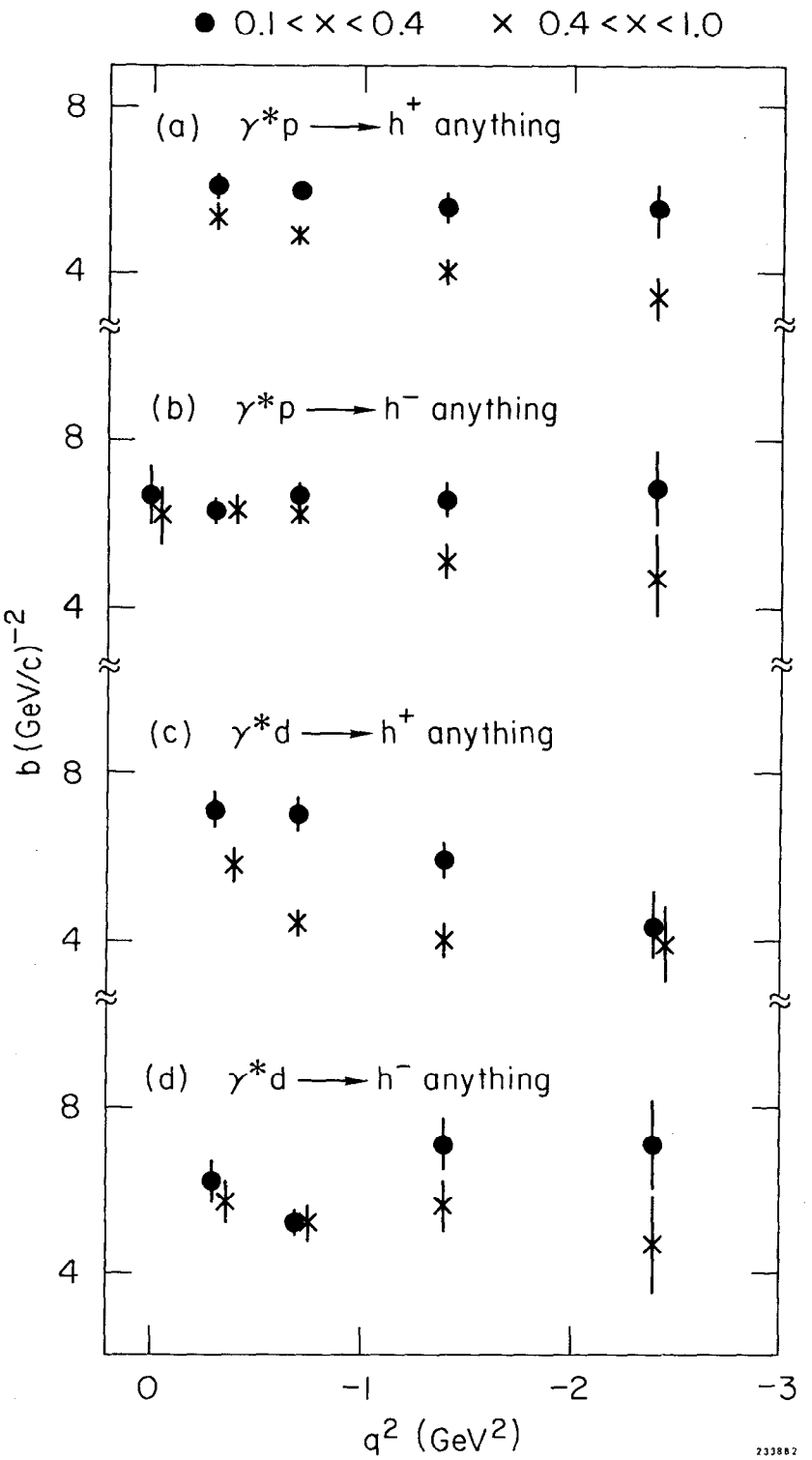
● 0.1 < x < 0.4 × 0.4 < x < 1.0
(a) γ*p → h+ anything
(b) γ*p → h− anything
(c) γ*d → h+ anything
(d) γ*d → h− anything
b (GeV/c)−2
8
4
0
−1
−2
−3
q2 (GeV2)
233882

Fig. 32

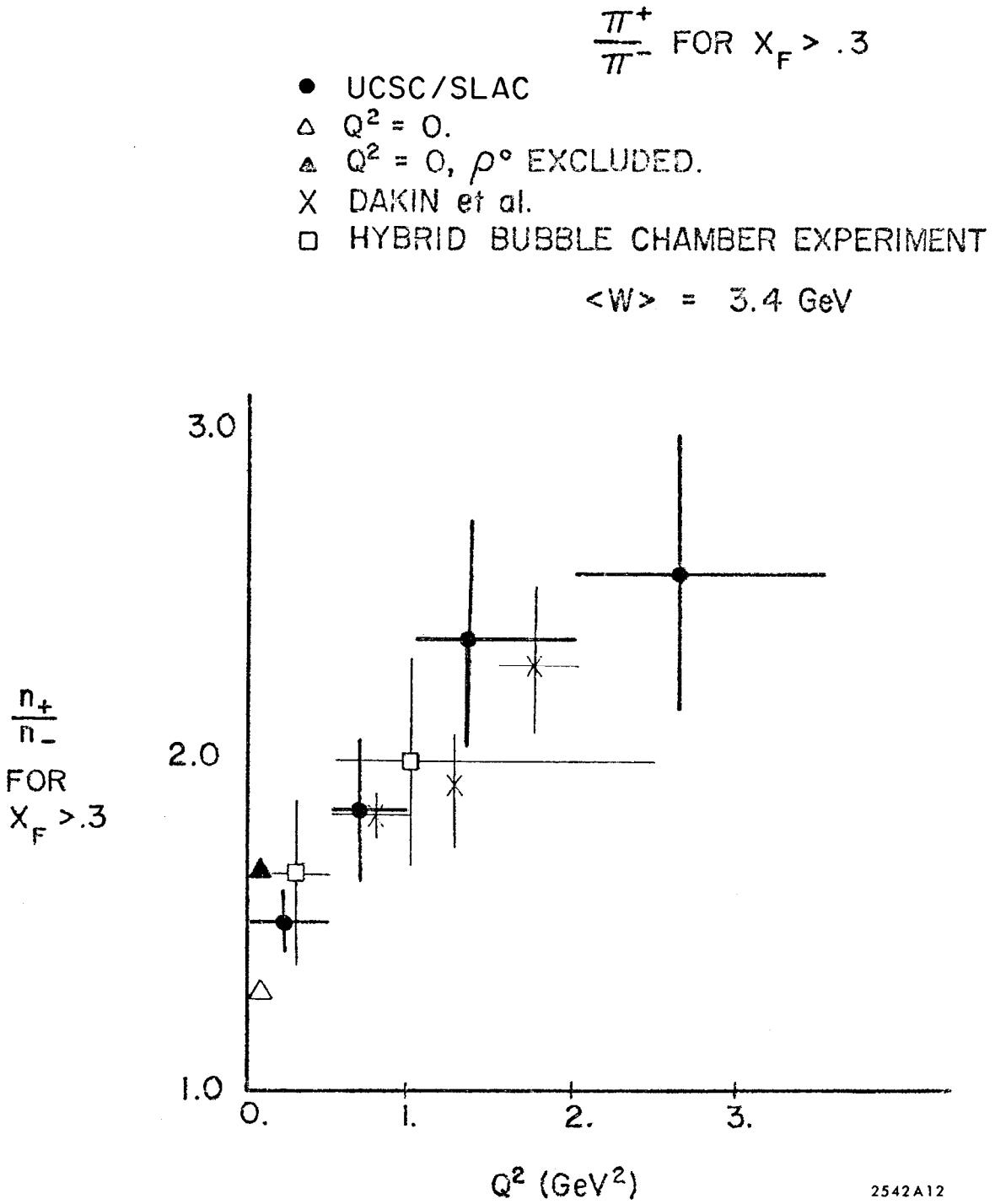
$\frac{\pi^+}{\pi^-}$ FOR $X_F > .3$
● UCSC/SLAC
△ $Q^2 = 0.$
▲ $Q^2 = 0$, ρ° EXCLUDED.
X DAKIN et al.
□ HYBRID BUBBLE CHAMBER EXPERIMENT
$\langle W \rangle = 3.4$ GeV
$\frac{n_+}{n_-}$ FOR $X_F > .3$
3.0
2.0
1.0
0.
1.
2.
3.
Q^2 (GeV^2)
2542A12

Fig. 33

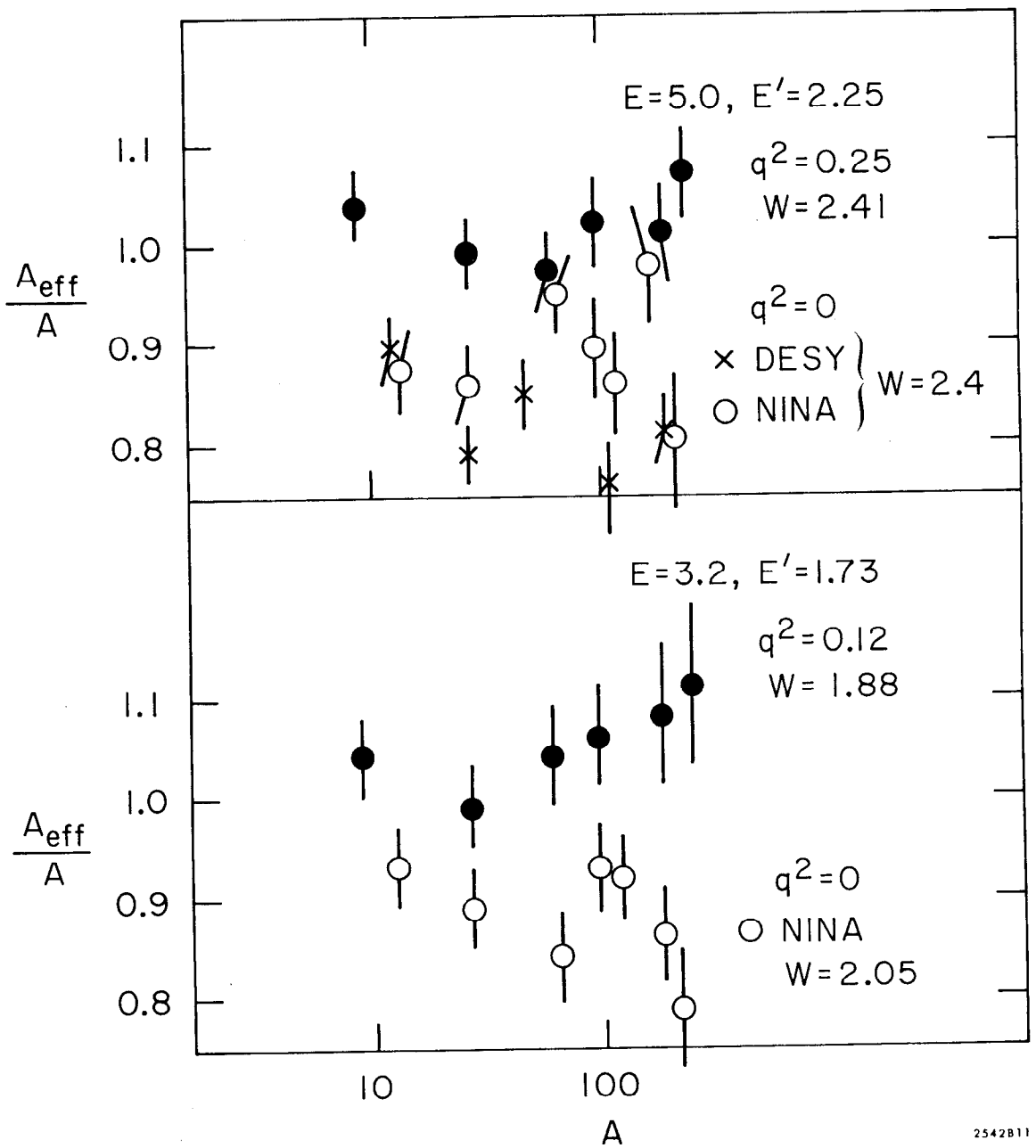
E=5.0, E′=2.25
q2=0.25
W=2.41
q2=0
× DESY
O NINA
W=2.4
E=3.2, E′=1.73
q2=0.12
W= 1.88
q2=0
O NINA
W=2.05
Aeff/A
1.1
1.0
0.9
0.8
10
100
A
2542B11

Fig. 34

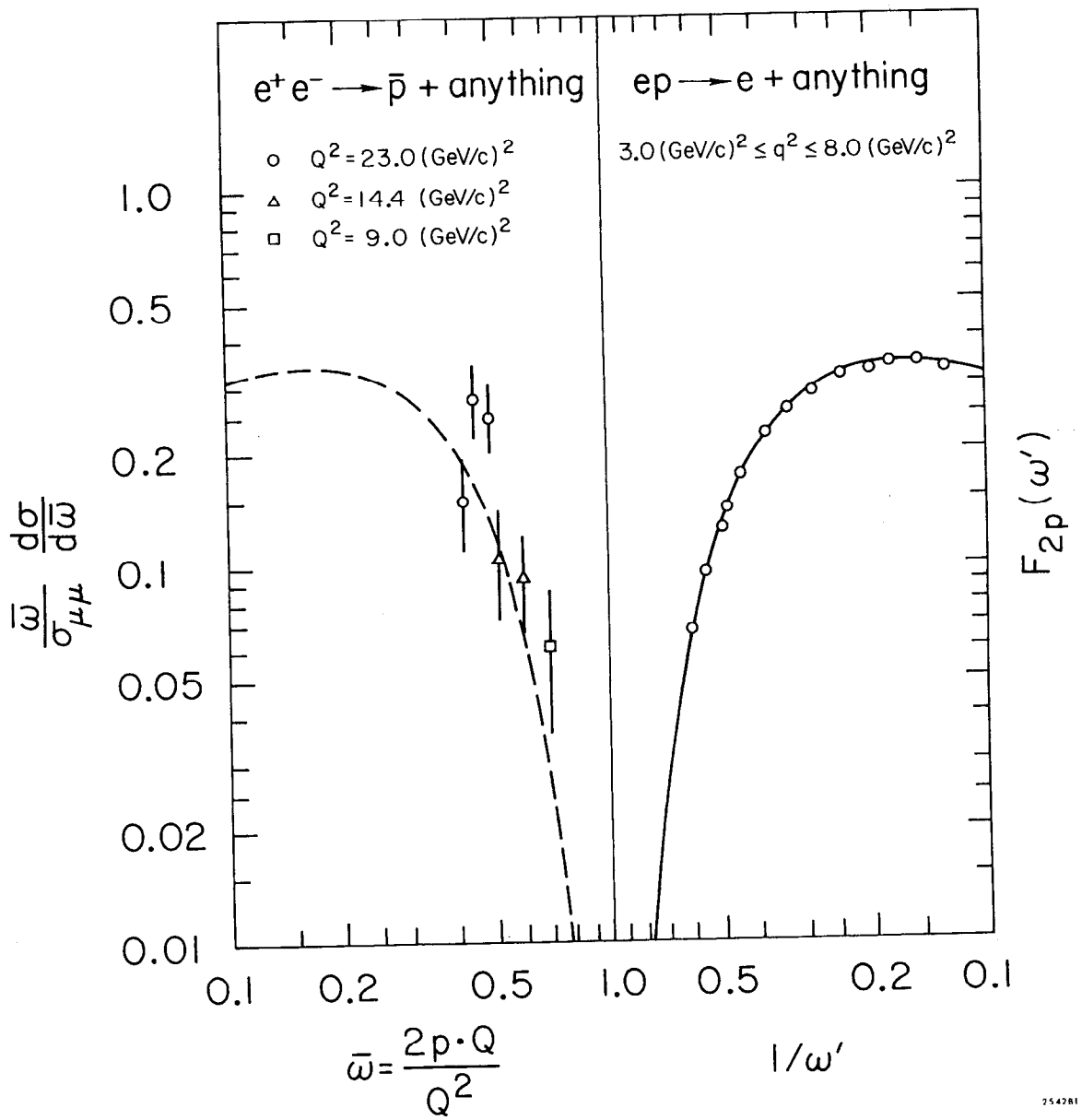
e+ e− → p̄ + anything
ep → e + anything
Q2 = 23.0 (GeV/c)2
Q2 = 14.4 (GeV/c)2
Q2 = 9.0 (GeV/c)2
3.0 (GeV/c)2 ≤ q2 ≤ 8.0 (GeV/c)2
1.0
0.5
0.2
0.1
0.05
0.02
0.01
0.1
0.2
0.5
1.0
0.5
0.2
0.1
ω̄ = 2p·Q / Q2
1/ω′
F2p (ω′)
254281

Fig. 35

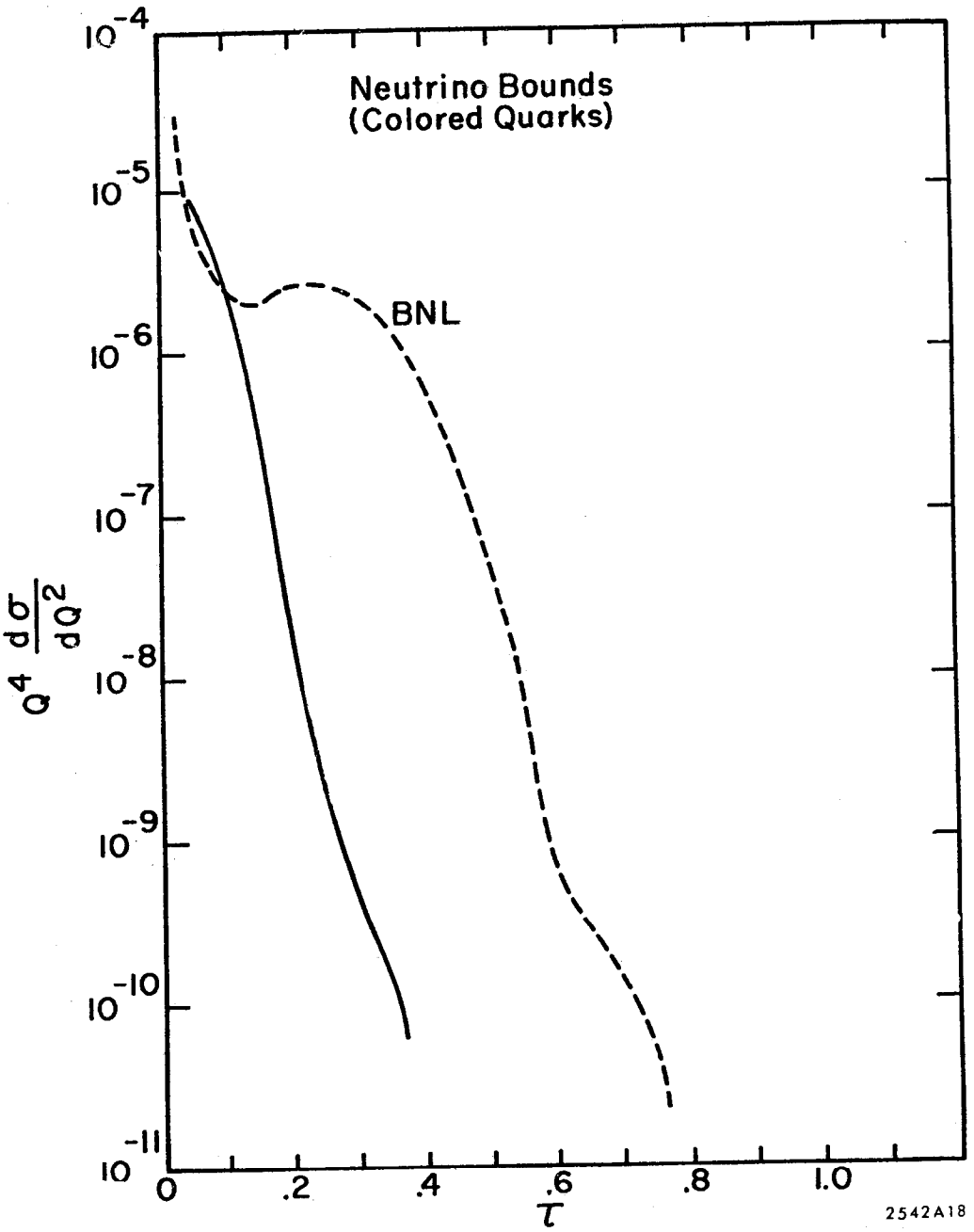
Neutrino Bounds
(Colored Quarks)
BNL
10^{-4}
10^{-5}
10^{-6}
10^{-7}
10^{-8}
10^{-9}
10^{-10}
10^{-11}
$Q^4 \frac{d\sigma}{dQ^2}$
0
.2
.4
.6
.8
1.0
τ
2542A18

Fig. 36

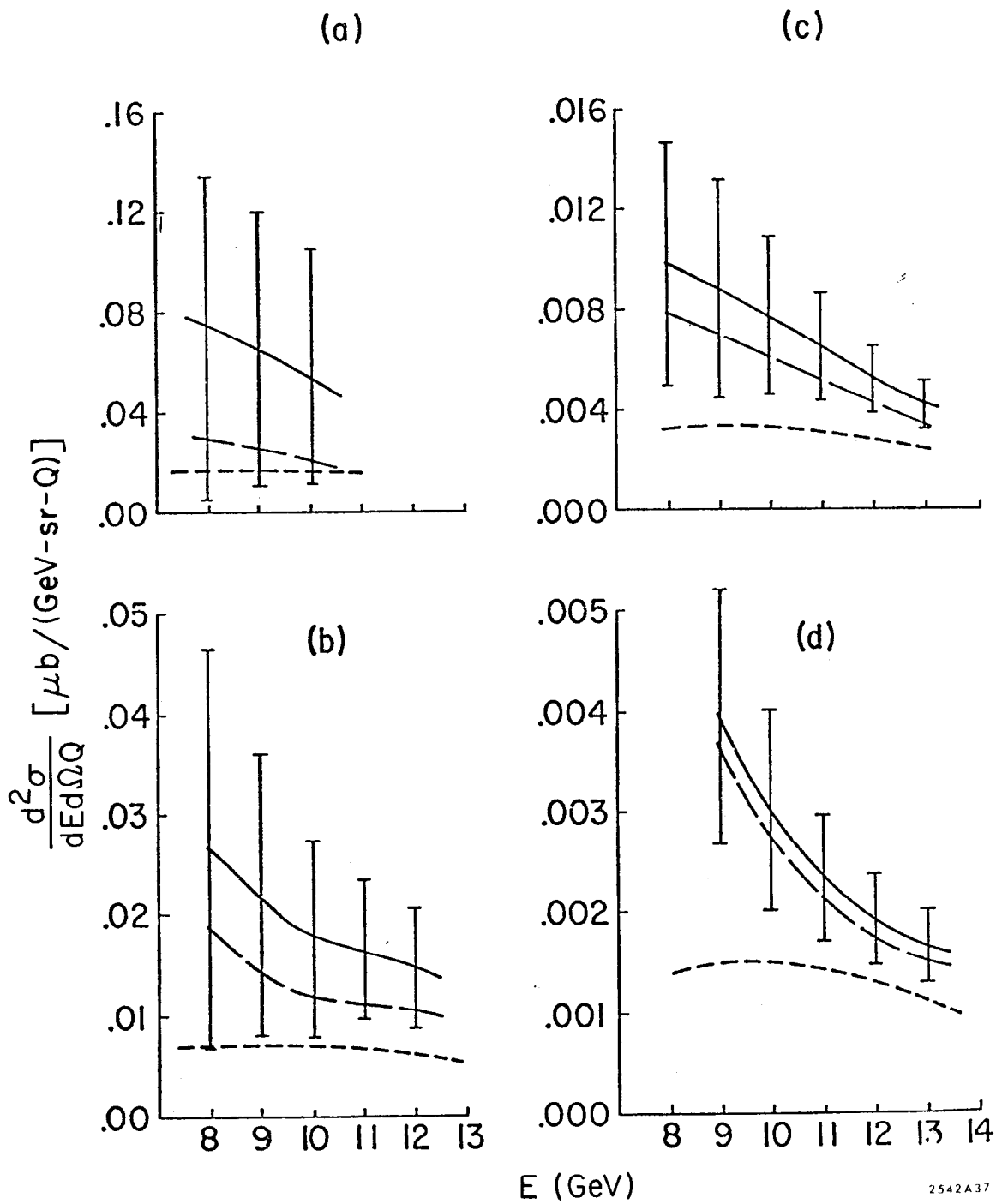
(a)
(c)
(b)
(d)
.16
.12
.08
.04
.00
.016
.012
.008
.004
.000
.05
.04
.03
.02
.01
.00
.005
.004
.003
.002
.001
.000
8 9 10 11 12 13
8 9 10 11 12 13 14
E (GeV)
$\frac{d^2\sigma}{dEd\Omega Q}$ [μb/(GeV-sr-Q)]
2542A37

Fig. 37